FRAGMENTATIONS OF AND ENERGY DEPOSITION IN MOLECULAR IONS OF 4-METHOXYBENZIL-d_5 AND BENZIL PRODUCED BY ELECTRON IMPACT

By

JON ALAN DRAEGER

Bachelor of Science

Northeastern Oklahoma State University

Tahlequah, Oklahoma

1971

Submitted to the Faculty of the Graduate College
of the Oklahoma State University
in partial fulfillment of the requirements
for the Degree of
MASTER OF SCIENCE
July, 1975

FRAGMENTATIONS OF AND ENERGY DEPOSITION IN MOLECULAR IONS OF 4-METHOXYBENZIL-d_5 AND BENZIL PRODUCED BY ELECTRON IMPACT

Thesis Approved:

Stuart E. Scheppele
Thesis Adviser

Robert J. Moore

J. Paul Devlin

N. N. Durham
Dean of the Graduate College

To L. E. L. and J. L. N.

ACKNOWLEDGEMENTS

I wish to thank Dr. Stuart E. Scheppele for his guidance and encouragement throughout the course of this study. I would like to acknowledge my advisory committee: Drs. J. Paul Devlin, Lionel M. Raff, Gilbert J. Mains, and Joel J. Martin.

I am indebted to Dow Chemical Company and Oklahoma State University for financial assistance, and wish to acknowledge the many hours of discussions with my colleagues.

I would like to thank Wayne Atkins for the repair of equipment necessary for this study.

TABLE OF CONTENTS

LIST OF TABLES

LIST OF FIGURES

LIST OF FIGURES (Continued)

CHAPTER I

INTRODUCTION

The assumption that a mass spectrum of polyatomic molecules result from competitive and consecutive unimolecular reactions of internally excited molecular ions was used in the development of quasi-equilibrium theory (QET) by Rosenstock, Wahrhaftig, and Eyring.[1] In accordance with this theory, a calculated mass spectrum can be obtained by folding a breakdown graph into an internal energy distribution function, P(E).[2] The breakdown graph is constructed from the RRKM rate constants, $k_i(E)$, for the unimolecular decompositions and the various resident times in the mass spectrometer. The $k_i(E)$ are calculated as a function of the internal energy of the molecular ion. Prediction and/or analysis of a mass spectrum thus requires knowledge of the rate constants, $k_i(E)$, and of P(E).

Following Morrison, the ion intensity at any nominal voltage V with a spread in energies given by m(U) is given by Equation 1.[3]

$$I(V)= \int_{Ec}^{\infty} \sum_{k=1}^{j} K_k(E_i-E_{c,k})^n \, m(E_i-V) \, dE_i \qquad (1)$$

where K_k is the probability for transition from a specific state of the neutral molecule to a specific level of the molecular ion, $(E_i-E_{c,k})^n$ is the threshold law for the transition, and the total electron energy $E_i=U+V$ with U being the thermal energy of the electrons. The value of the exponent n in the threshold law is taken as 1 and 0 for single

direct ionization by electrons and photons, respectively.

The n+1 derivative of the ion intensity evaluated at $E_i=E_c$ is given in Equation 2.[3]

$$d^{n+1}/dV^{n+1} = -\Sigma\ K_k\ m(V-E_c) \qquad (2)$$

Therefore, the appropriate derivative of the total ionization reduces to the transition probabilities convoluted with the electron energy distribution, reversed with respect to the energy axis.

Chupka has shown that the second (first) derivatives of the ionization efficiency of the various ions produced by electron impact on (photoionization of) the neutral molecule normalized by their sum gives an approximation to the breakdown graph.[4] Experimental breakdown graphs can also be obtained from charge exchange reactions[5] and from photoion-photoelectron coincidence mass spectrometry.[6]

Within the limits of a linear threshold law for single direct ionization by electrons (a step-function for ionization by photons), Equation 2 shows that the second (first for photoionization) derivative of the total ionization efficiency times the function $(V-E_i)$, where E_i is the internal energy of the ions, gives the distribution of the transition probabilities. This distribution is termed the energy deposition function, P(ED),[7,8] and is the energy deposited in the molecular ion during the ionization event. It has been shown that the P(ED) function when folded into the thermal energy distribution of the neutral molecule at a gas temperature T gives an approximation to the internal energy distribution function, P(E).[9]

A substituent may affect the yield of the various ions by its affect on a) the internal energy distribution function, b) the primary

reaction rates, and c) the secondary reaction rates.[10] A preliminary study of a series of benzils indicated that the RRKM rate constants for the formation of substituted benzoyl ions relative to those for the formation of unsubstituted benzoyl ions showed Hammett correlation, and that rho decreased with increasing excitation energy.[11] To provide a more definitive basis for this conclusion a detailed study of the electron impact induced ionization-fragmentation of 4-methoxybenzil-$\underline{d}_5$ (1-phenyl-$\underline{d}_5$-2-(4-methoxyphenyl)ethane-1,2-dione) at an ion source temperature of 250° C was undertaken. Also the study of benzil (1,2-diphenylethane-1,2-dione) has been extended to include measurements at an ion source temperature of 310° C. Equations for the analysis of the error in dI/dE and d^2I/dE^2 contributed by shot noise are included in this thesis. A logic diagram and a discussion of the subroutines used in the processing of the experimental dI/dE are presented.

CHAPTER II

RESULTS AND DISCUSSION

Xenon

The electron energy was calibrated with the ionization potential of Xenon. The dI/dE data of Xenon was differentiated without smoothing and the first maximum was taken as the ionization potential ($\sim$12.15 eV[12]). The full width at half maximum (FWHM) in the d^2I/dE^2 data, 0.59±0.03 eV, reflects the energy spread in the ionizing electron beam.

The d^2I/dE^2 curve of Xenon in Figure 1 showed particular fine structure. The peaks observed in this curve are compared with the results of previous spectroscopic[13] and electron impact[14,15] investigations in Table I. Maxima in the d^2I/dE^2 curve at 12.45, 12.85, and 13.30 eV correlate well with autoionization levels observed from spectroscopy (Huffman) and the results of Marmet and Johnstone. Other maxima at $\sim$13.03, $\sim$13.16, and $\sim$13.23 eV are not observable due to the energy resolution of the electron beam.

The photoionization efficiency curve of Xenon is presented in Figure 2.[16] The intensity of the $^2P_{3/2}$ state is small compared to the intensity of the 6d' autoionization level. This result was observed by Dibler, et. al.,[17] and by Marmet. Given the FWHM in the electron energy distribution and the energy spacings in Table I, Equation 2 reveals that in general adjacent bands in the d^2I/dE^2 curve for Xenon

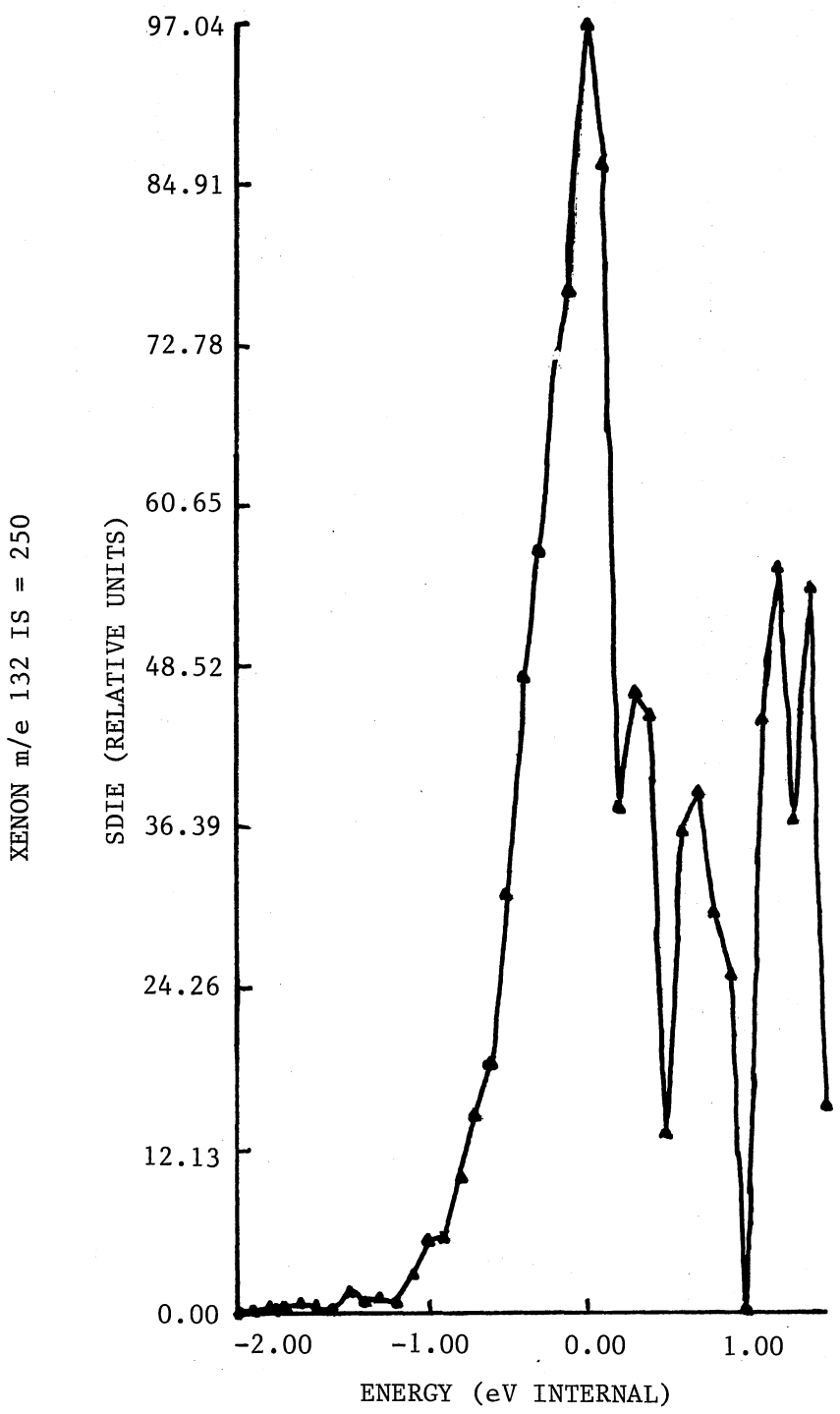

Figure 1. d^2I/dE^2 for Xenon

TABLE I

ELECTRON STATES OF XENON

Marmet[a]	Johnstone[b]	Huffman[c]	Configuration[c]	This Work[d]
12.127	12.09	12.15	$^2P_{3/2}$	12.15[e]
	12.27			
12.439	12.41	12.47	6d'	12.45
12.799	12.80	12.85	7d'	12.85
13.039	13.04	13.03	8d'	
13.159	13.16	13.16	9d'	
		13.23	10d'	
		13.27	11d'	13.30
	13.53	13.47	$^2P_{1/2}$	13.55

[a]Electron Impact, Reference 14

[b]Electron Impact, EDD Method, Reference 15

[c]Photo Absorption, Reference 13

[d]Average of two curves (SDIE)

[e]Assigned

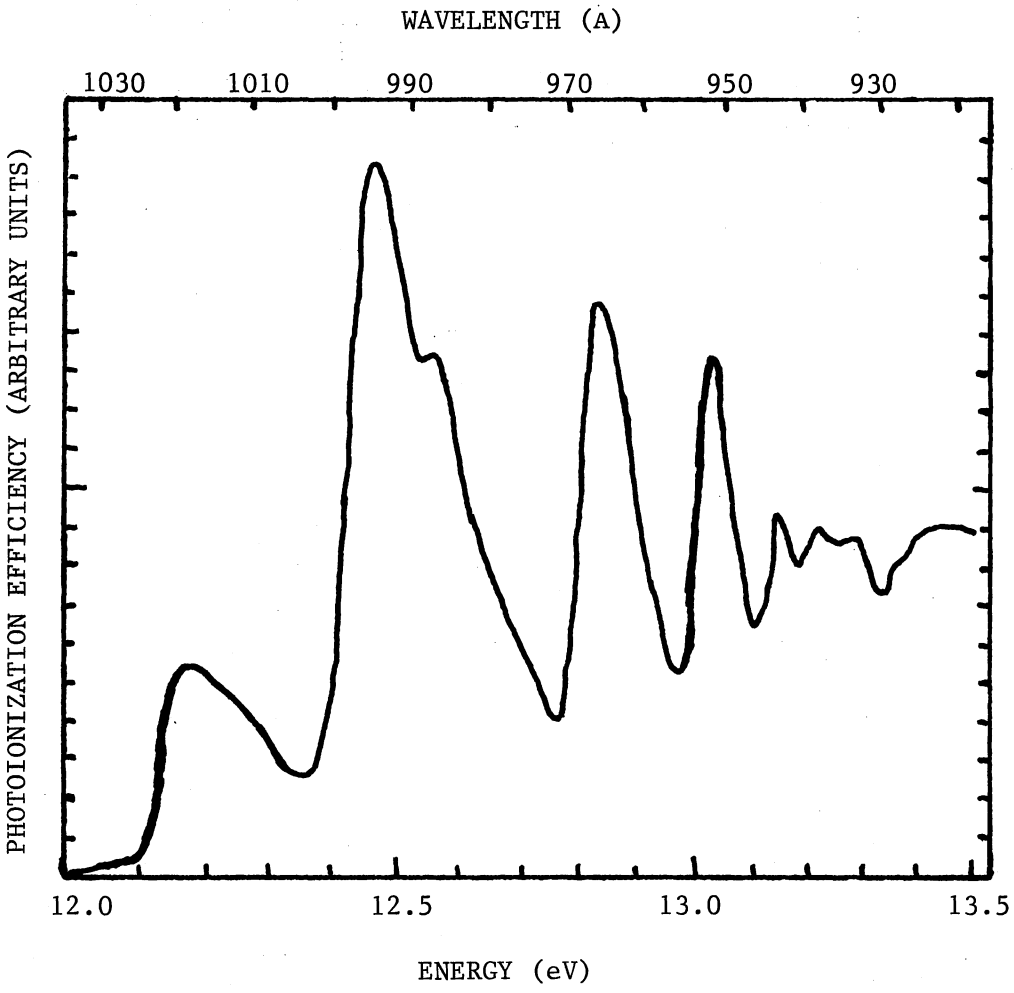

Figure 2. Photoionization Efficiency Curve of Xenon

will not be fully resolved. Because the d^2I/dE^2 curve in Figure 1 will reflect to some extent the sum of overlapping Gaussian distributions 1) no attempt was made to compare the relative peak heights with known relative transition probabilities, and 2) the error in calibrating the energy must be $0 \leq E \leq 0.3$ eV.

Thus these conclusions suggest a maximum error of 0.3 eV, which is not excessive for the experimental apparatus used. Conventional electron impact ion sources give ionization potentials to ±0.1 eV. Positive identification, however, could be made from improved energy resolution of the electron beam, by use of other substances for calibration, or from a comparison with the convolution of transition probabilities for Xenon with an electron energy distribution having a FWHM of 0.6 eV.

4-Methoxybenzil-$\underline{d}_5$

Fragmentation Scheme

The 70 eV mass spectrum of 4-methoxybenzil is reproduced in Figure 3.[18] The molecular ion, m/e 240, fragments to form either the 4-methoxybenzoyl ion, m/e 135, or the benzoyl ion, m/e 105.[11] These ions further fragment by the loss of CO to form ions at m/e 107 and m/e 77, respectively. The m/e 107 ion loses H_2CO, also forming the $C_6H_5^+$ ion.

To study the fragmentation of the m/e 105 and m/e 107 ions, the unsubstituted ring was labeled with five deuteriums. The reactions are then m/e 110 → m/e 82 + CO and m/e 107 → m/e 77 + H_2CO, respectively. The ion abundances in Table II show that the 70 eV mass spectrum of 4-methoxybenzil-$\underline{d}_5$ (I) is dominated by nine ions. Metastable peaks

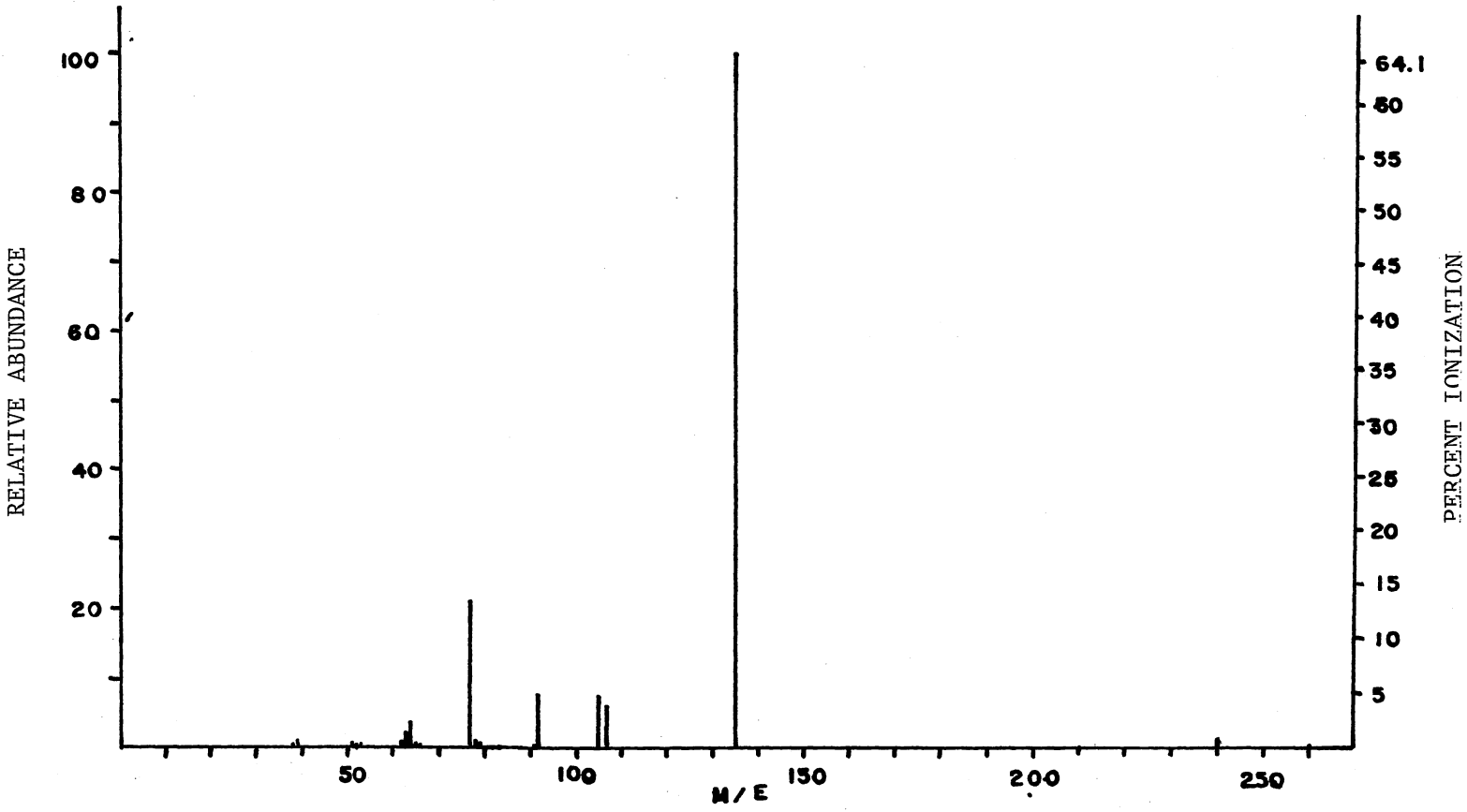

Figure 3. 70 eV Mass Spectrum of 4-Methoxybenzil

TABLE II

PERCENT ION ABUNDANCES IN THE MASS SPECTRA OF 4-METHOXYBENZIL-d_5 AS A FUNCTION OF ELECTRON ENERGY

	m/e										
eV	245	135	110	107	92	82	77	64	54	51	Total
13.39	1.6	97.3	0.9	0.2	0.0	0.0	0.0	0.0	0.0	0.0	100%
15.19	1.4	95.6	1.7	1.2	0.0	0.0	0.1	0.0	0.0	0.0	100%
20.6	1.0	82.6	3.4	4.6	1.1	1.1	3.7	0.0	0.0	0.0	97.5%
70	0.7	60.6	4.4	5.0	3.9	5.6	6.5	2.1	2.4	0.4	91.6%

were observed for the following transitions: m/e 135 → m/e 107 + 28 (m*= 84.8), m/e 110 → m/e 82 + 28 (m*= 61.1), and m/e 107 → m/e 77 + 30 (m*= 55.5); and were not observed for the transitions m/e 245 → m/e 135 + 105 (m*= 74.4) or m/e 245 → m/e 110 + 135 (m*= 49.4). Scheme I (Figure 4), which is consistant with these data and results from related systems, is proposed to account for the mass spectrum of I.[8,19] Dissociation of C1-C2 bond in the molecular ion of I (II) produces either the 4-methoxybenzoyl ion, m/e 135 (III), or the benzoyl ion, m/e 110 (IV). These ions fragment with loss of CO to form ions with m/e 107 and m/e 82, respectively. The ion at m/e 77 is formed by subsequent fragmentation of m/e 107 with the loss of H_2CO. Other fragmentations are high energy processes and are not included in the study.

Derivatives of Ionization Efficiency

The FDIE curves, first derivative of the ionization efficiency curves, for ions II through VII are presented in Figures 5-10. In each figure, the points represent experimental dI/dE values. The curves extend 3-4 eV past their respective maxima. The theoretical and experimental percent standard deviations for three energies in the FDIE curve of each ion and Xenon are shown in Table III. The good correlation between the experimental standard deviation (σ_{est}) and the theoretical standard deviation (σ_{true}) provides evidence that the shot noise is the major contribution to the uncertainity in the experimental data.

The SDIE, second derivative of the ionization efficiency, curves of II through VII, with the d^2I/dE^2 points, are presented in Figures 11-16 as a function of the internal energy of the molecular ion of I

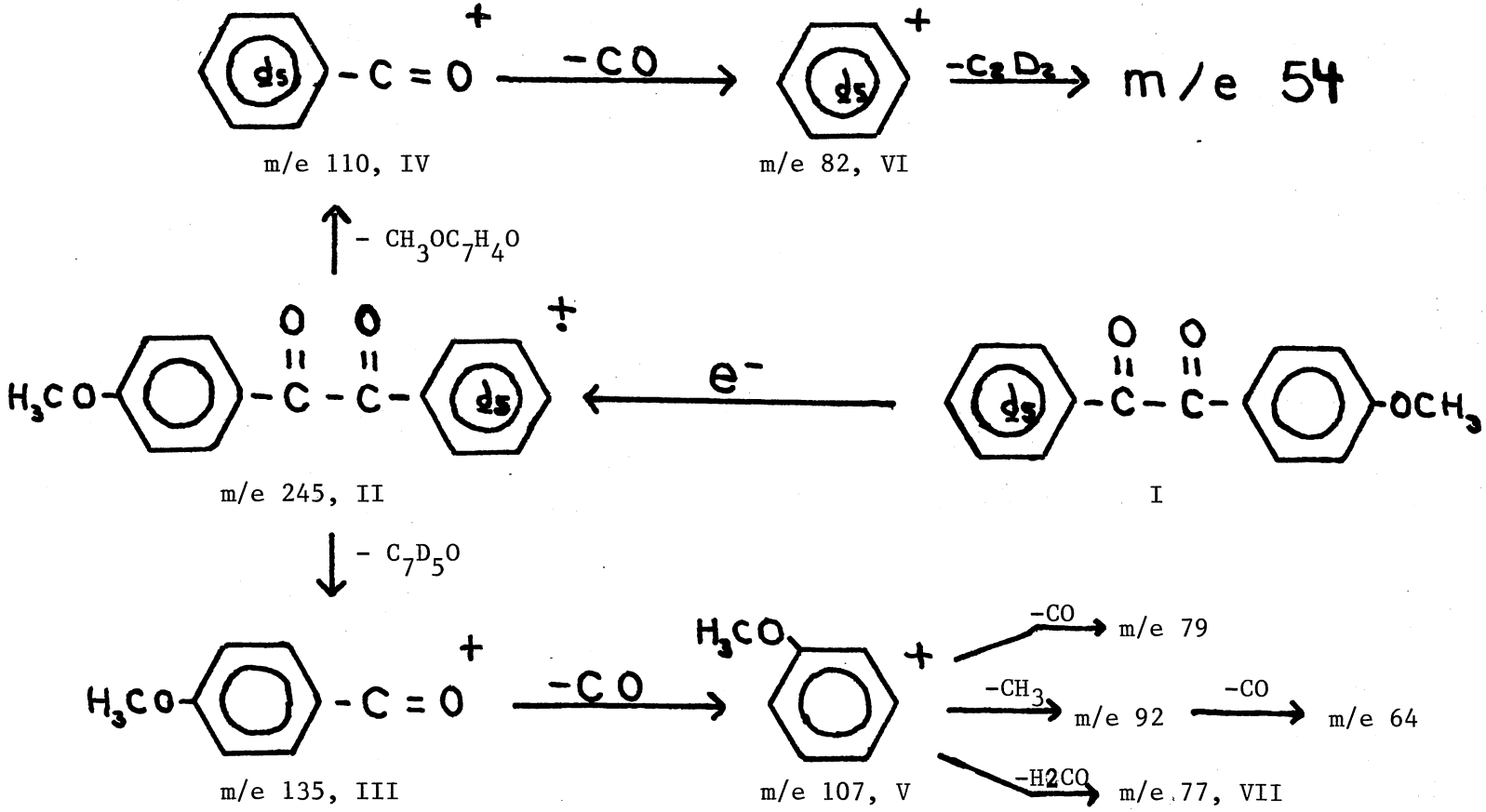

Figure 4. Scheme I. Detailed Fragmentation of 4-Methoxybenzil-$\underline{d}_5$

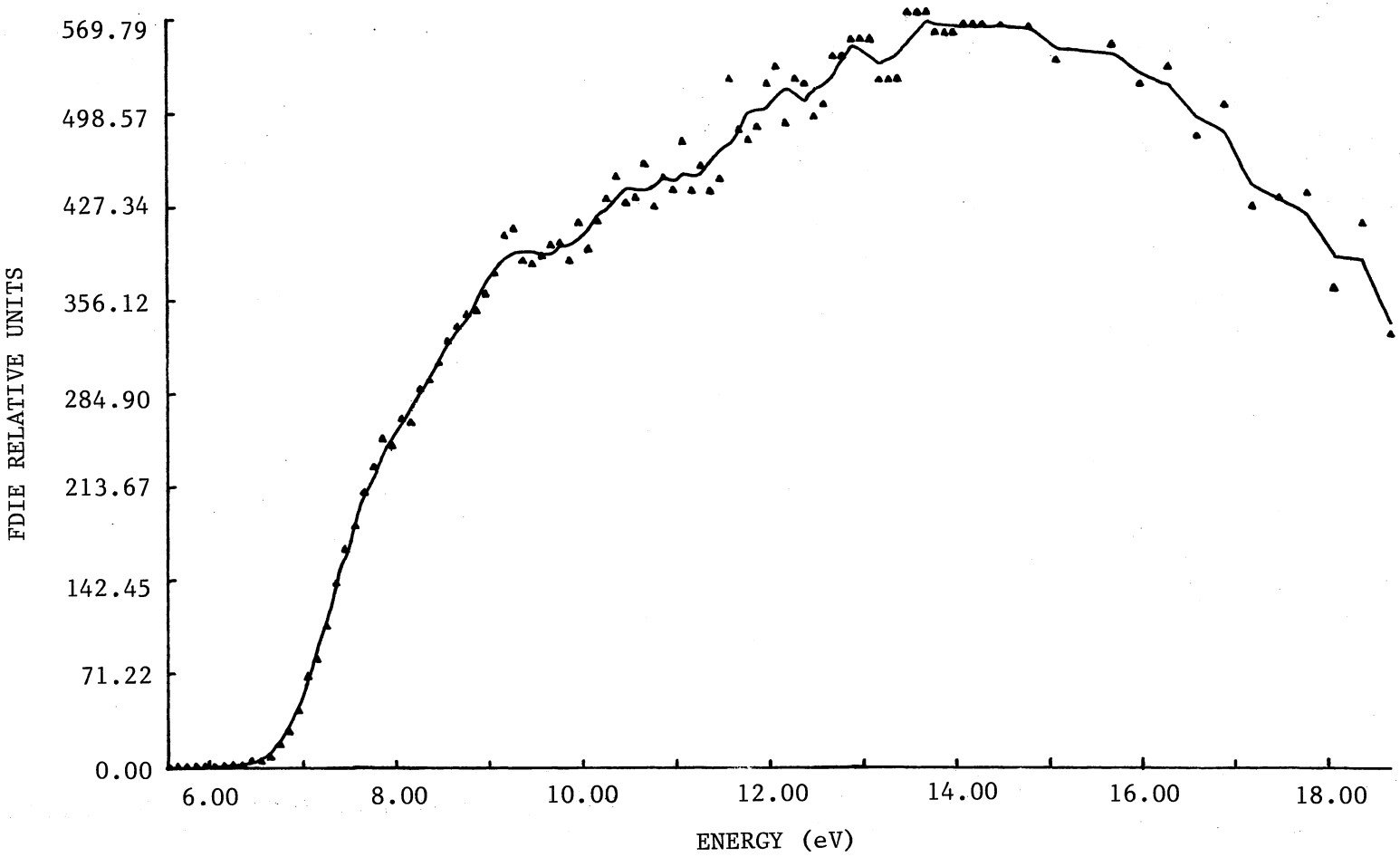

Figure 5. FDIE Curve of II, m/e 245

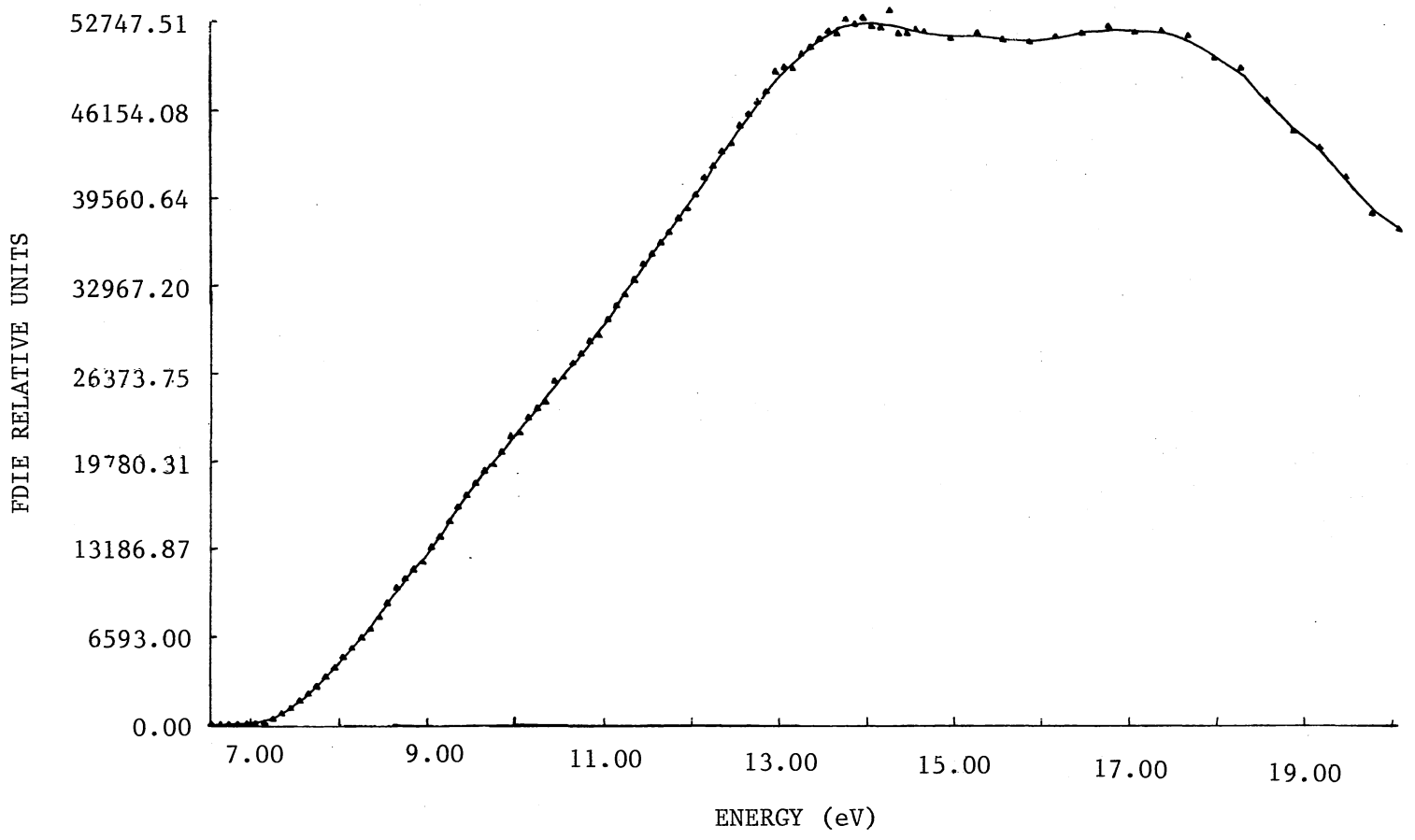

Figure 6. FDIE Curve of III, m/e 135

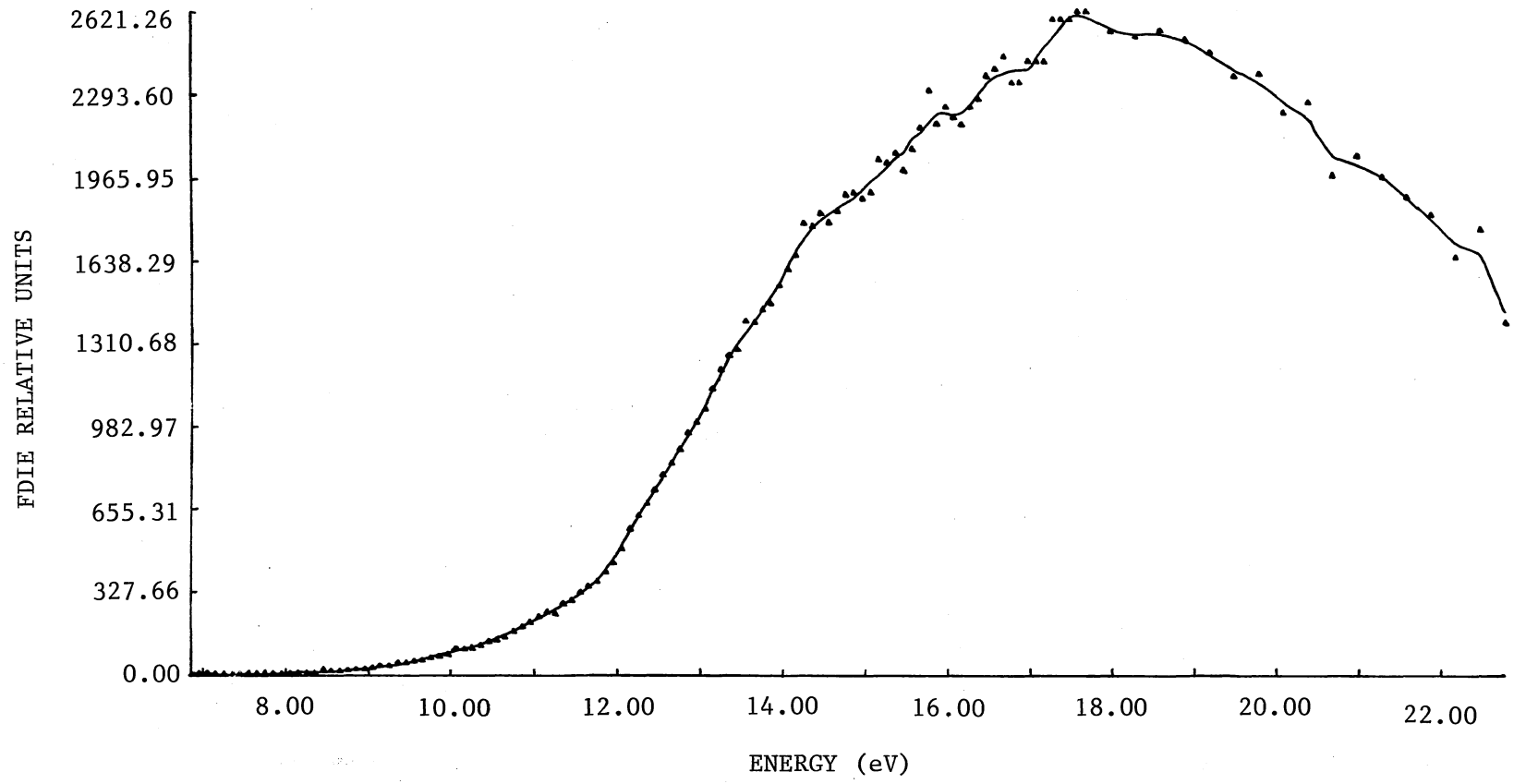

Figure 7. FDIE Curve of IV, m/e 110

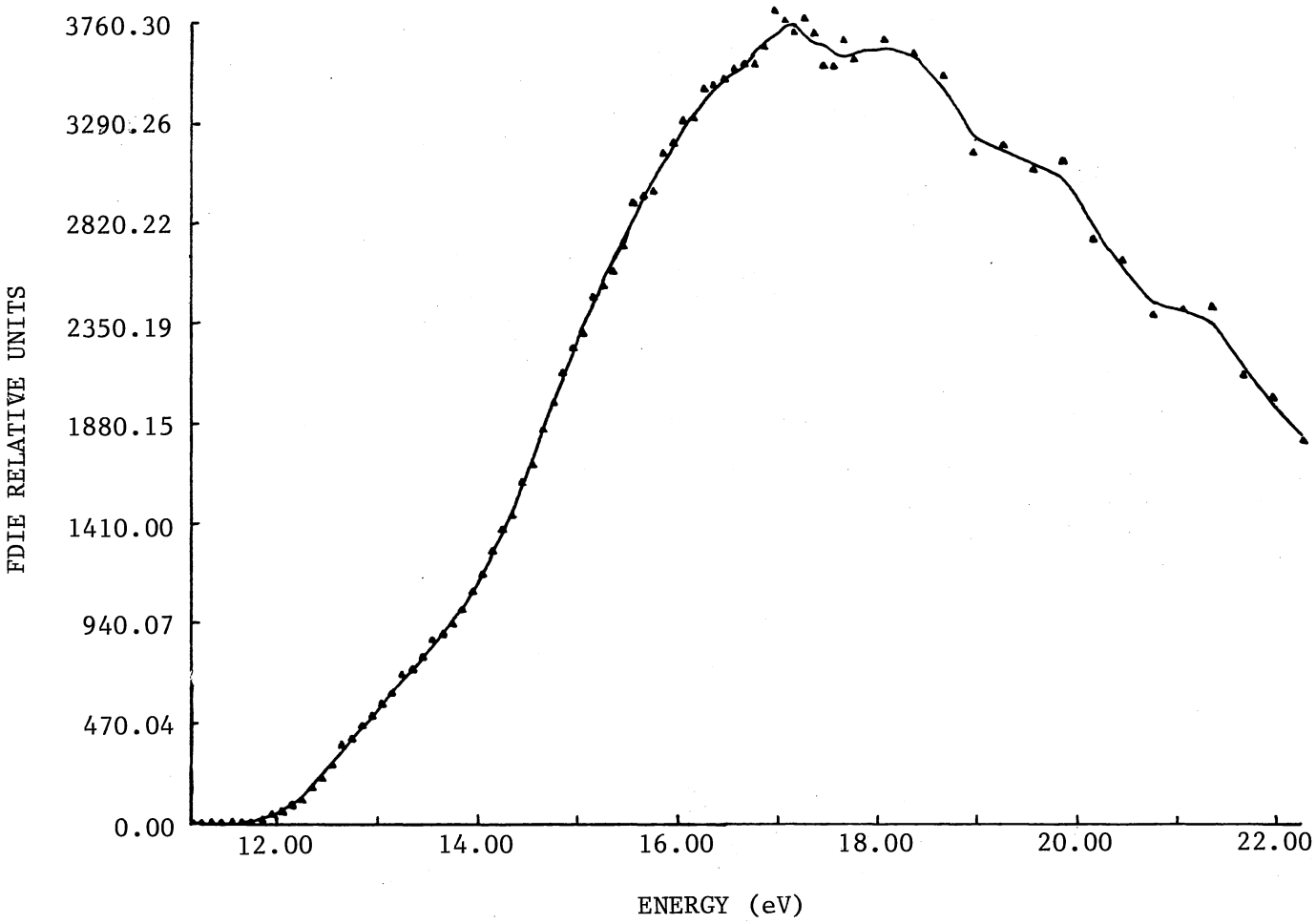

Figure 8. FDIE Curve of V, m/e 107

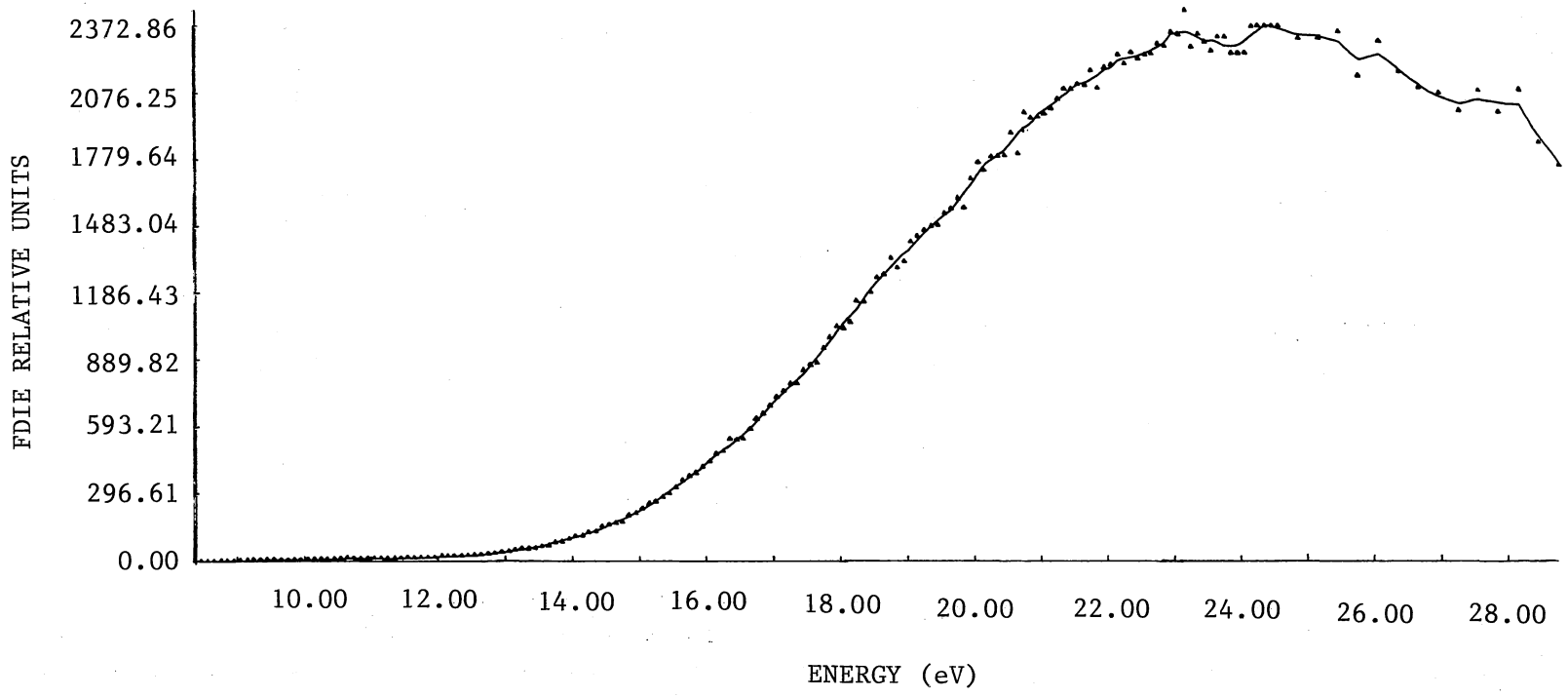

Figure 9. FDIE Curve of VI, m/e 82

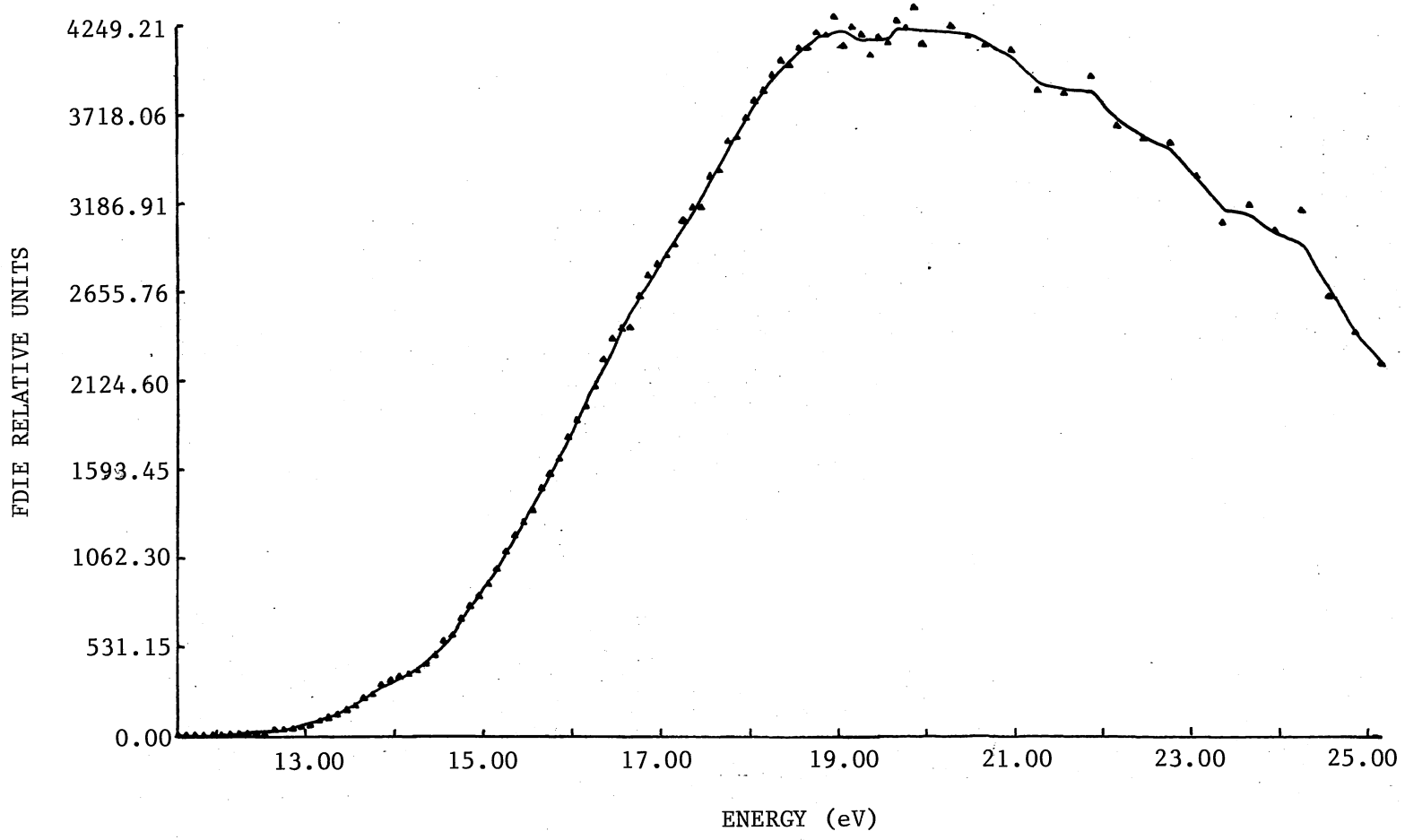

Figure 10. FDIE Curve of VII, m/e 77

TABLE III

STANDARD DEVIATIONS IN FDIE AND SDIE
OF 4-METHOXYBENZIL-d5
AND XENON

Ion m/e	eV[a]	$\%\sigma^{FDIE}_{true}$	$\%\sigma^{FDIE}_{est}$[b]	%σSDIE	Gain ($\times 10^{-4}$)
245	9.20	7.99	3.37	14.84	4.62
	9.90	8.02	2.71	26.22	3.34
	13.00	9.84	3.11	71.38	2.83
135	9.50	0.81	0.80	5.05	3.35
	11.70	1.71	0.69	8.03	3.51
	14.10	1.54	0.89	11.66	3.70
110	13.00	10.61	5.27	18.06	4.40
	15.50	4.57	5.07	19.53	3.40
	17.00	5.49	4.99	40.36	3.37
107	15.40	4.84	3.68	9.80	3.54
	17.00	3.46	2.96	13.91	3.52
	17.70	3.69	3.71	28.58	3.50
82	17.80	3.65	5.48	11.25	3.84
	20.30	5.17	4.20	32.80	3.52
	22.20	5.48	5.22	45.22	3.50
77	16.30	5.38	3.70	8.54	3.89
	19.00	3.73	2.94	17.46	3.65
	19.80	3.58	4.25	32.79	3.59
132	12.15	0.71	1.11	5.01	1.71
	12.85	0.79	0.74	5.35	1.68
	14.15	1.07	0.76	12.62	1.71

[a] Corrected

[b] For each ion the lock-in-amplifier time constant (sec.), integration time (sec.), and number of points taken to estimate σ are: m/e 245, 30,1,170; m/e 135,10,1,55; m/e 110,10,1,55; m/e 107,10,1,55; m/e 82, 10,1,55; m/e 77,10,1,55. The sampling interval was 11 seconds.

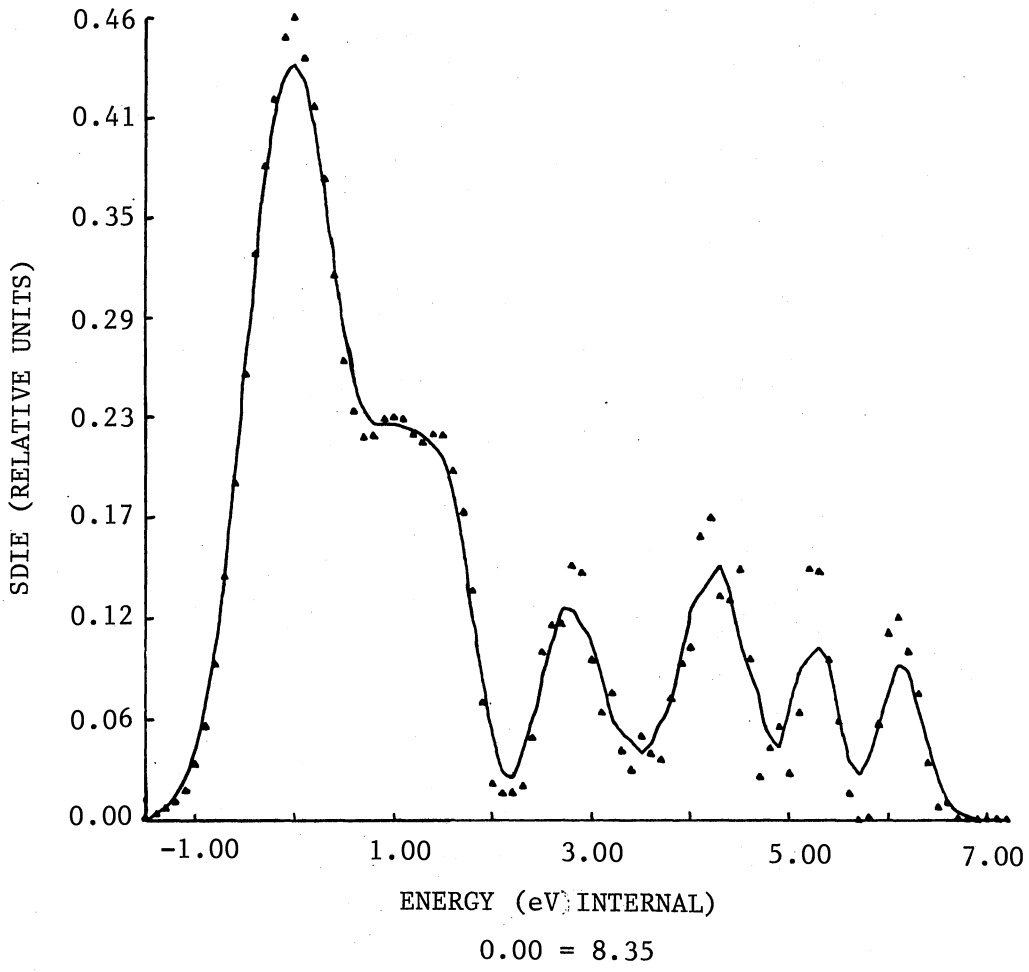

Figure 11. SDIE Curve of II, m/e 245

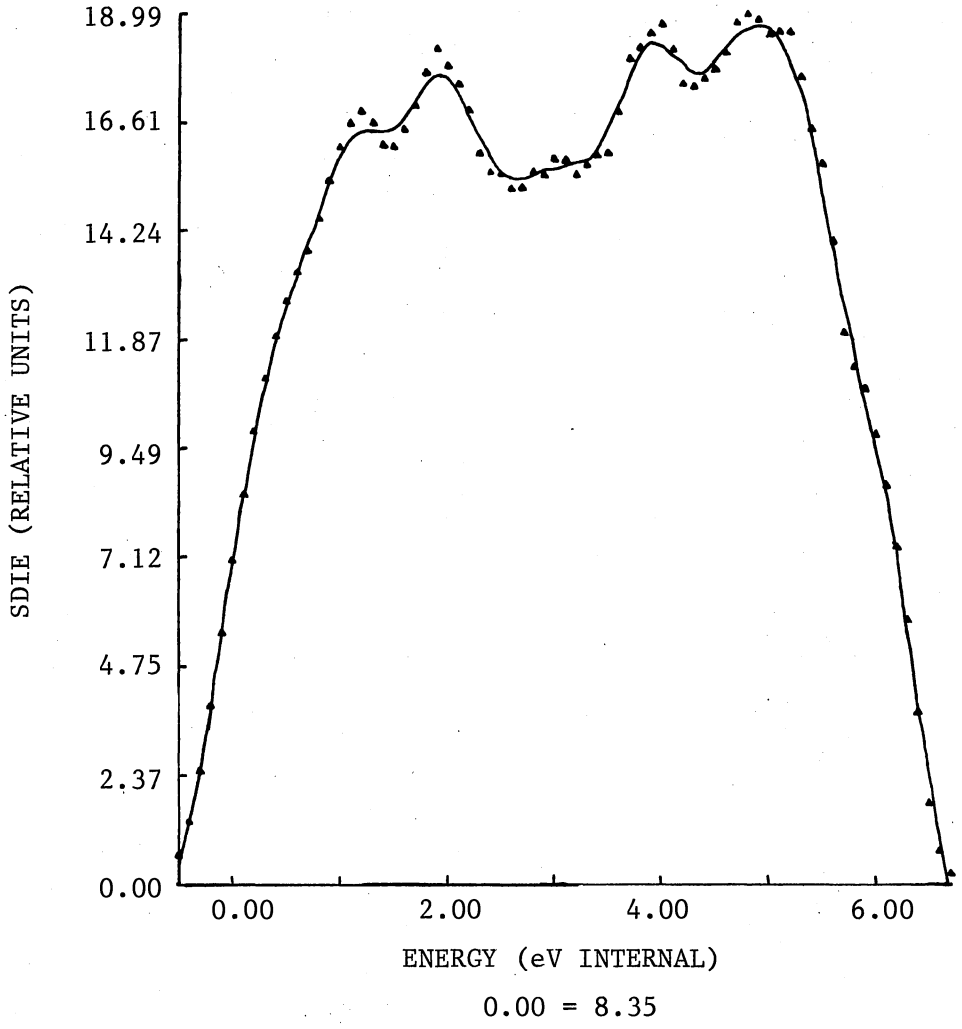

Figure 12. SDIE Curve of III, m/e 135

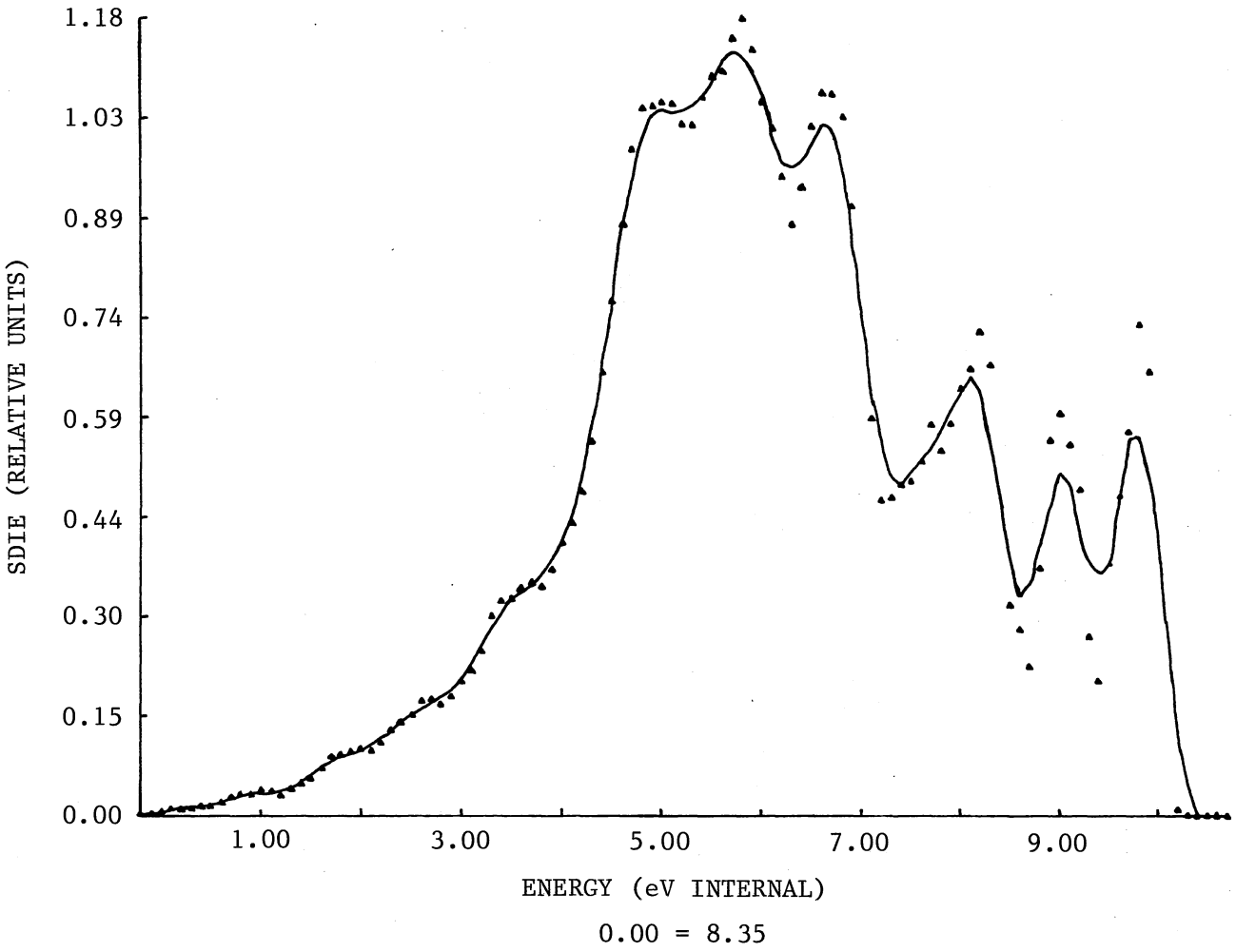

Figure 13. SDIE Curve of IV, m/e 110

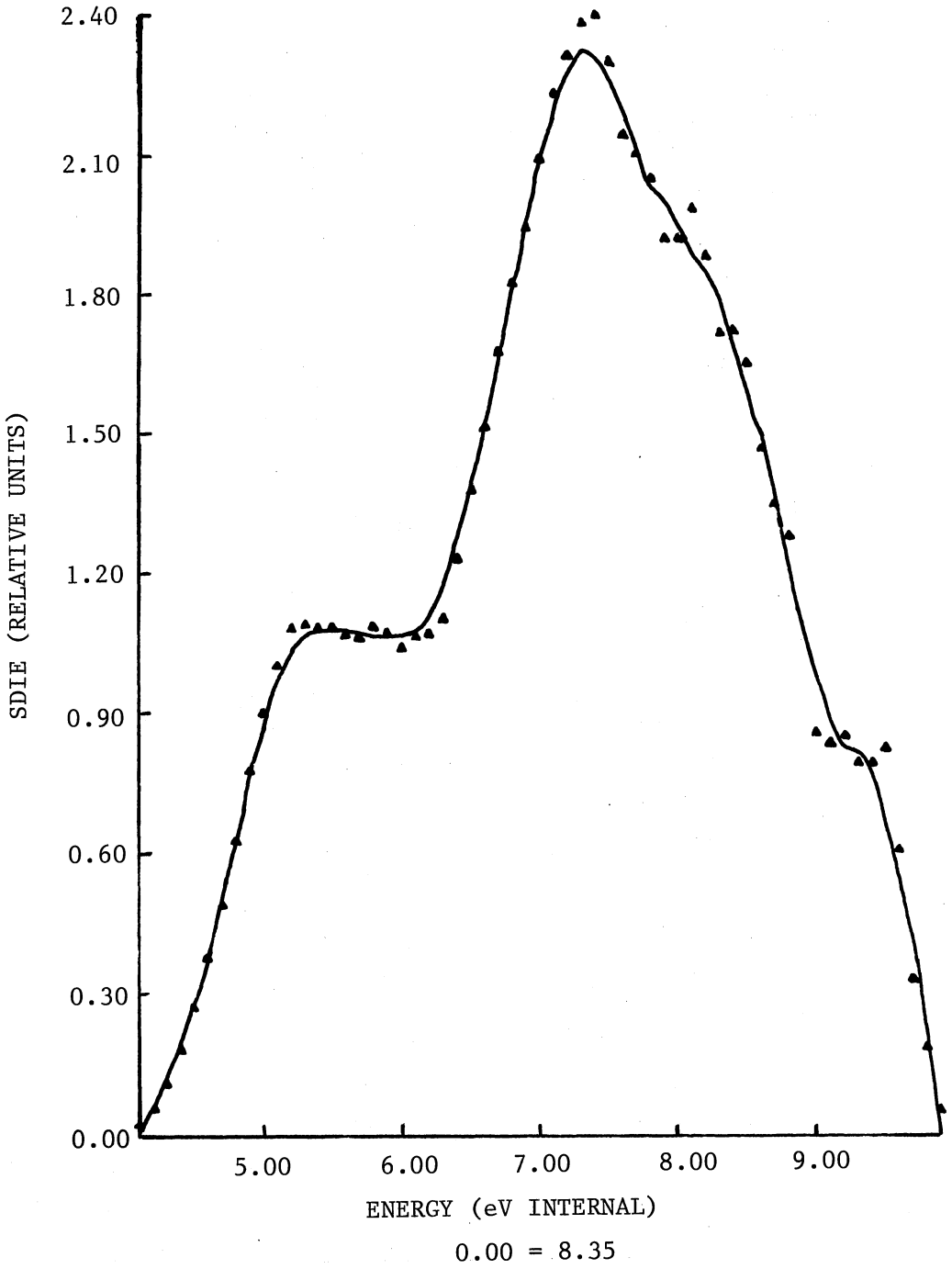

Figure 14. SDIE Curve of V, m/e 107

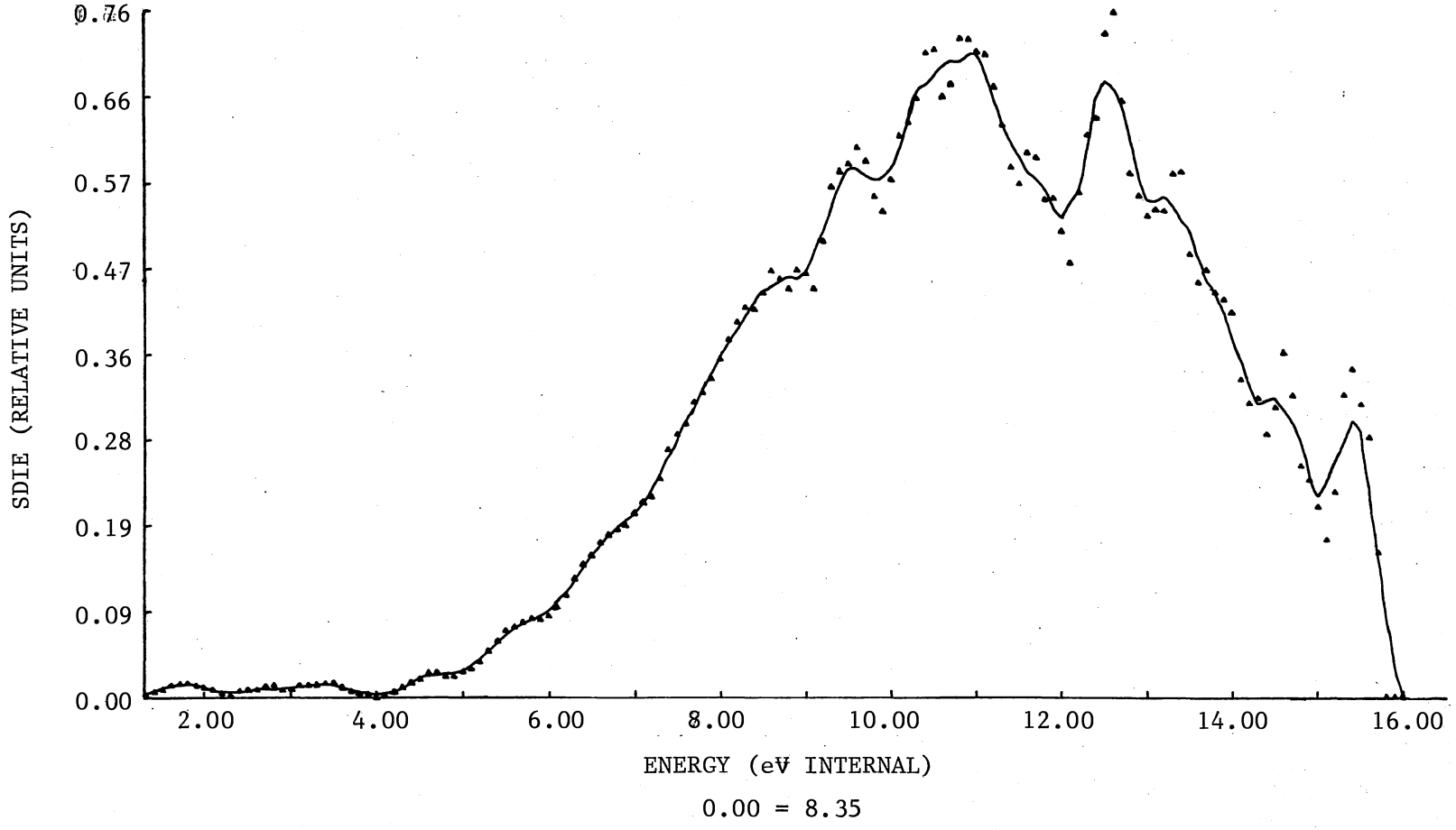

Figure 15. SDIE Curve of VI, m/e 82

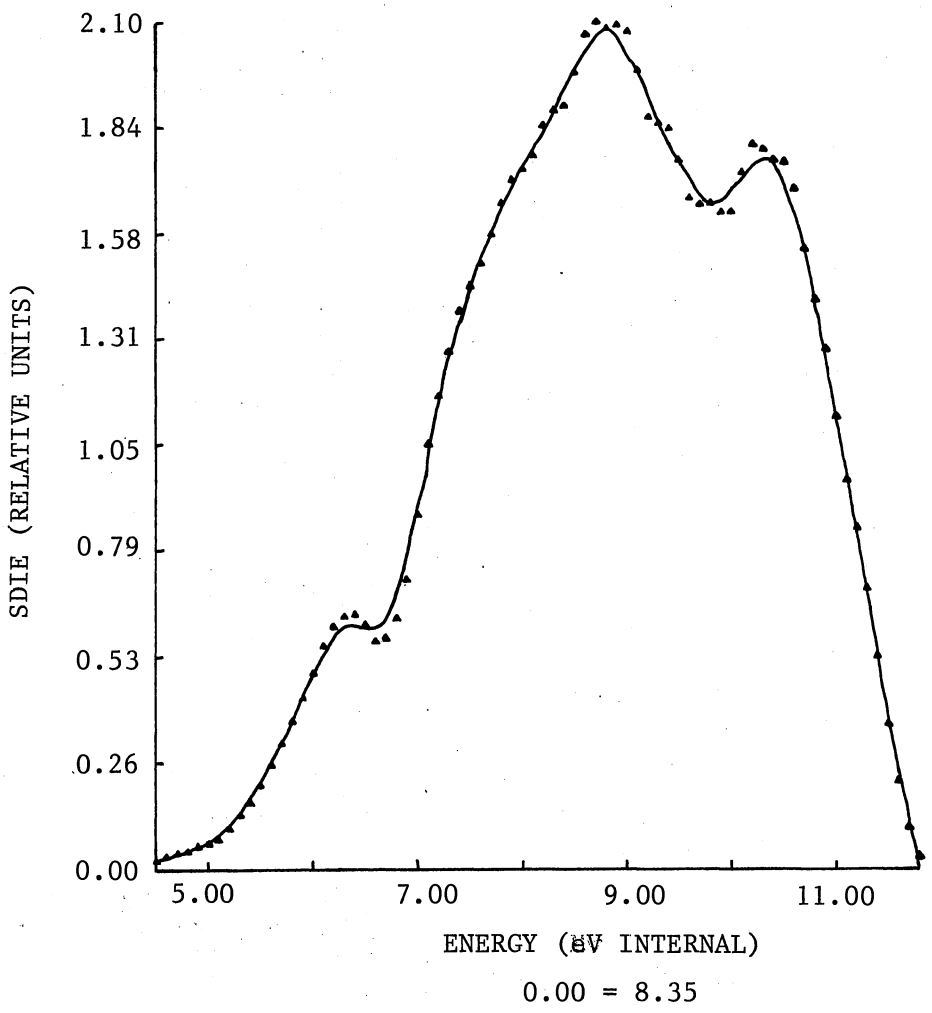

Figure 16. SDIE Curve of VII, m/e 77

(II). The internal energy is taken as the electron beam energy minus the ionization potential. The extension of the internal energy to negative values represents the effect of the electron energy distribution. The SDIE curve of the molecular ion (II) shows an ionization potential of 8.35 eV. This agrees reasonable well with the value of 8.14±0.20 eV calculated from thermodynamic considerations (see Apendix A). Conventional electron impact data can overestimate ionization potentials by as much as 0.3 eV.[20] Peaks appear in the SDIE curve of the molecular ion (II) at 2.80, 4.20, 5.20, and 6.10 eV of internal energy. Similiar maxima were observed in the SDIE curve of the molecular ion of 4-methylbenzil,[8] and are also observed in the SDIE curve of the molecular ion of benzil. These may reflect autoionizing states of the molecule or the formation of molecular ions in an excited electronic state. Interestingly, the photoelectron spectrum of benzil (Figure 17) shows peaks at 9.1 and 11.1 eV.[21] These results suggest that the higher maxima in the SDIE curve of II do not entirely result from autoionization.

Excess energy is often required for the dissociation rate constants, $k_i(E)$, to be in the region of 10^5-10^6 sec^{-1}. This excess energy is defined as the kinetic shift,[22] and thus the appearance potentials are upper linits of the true threshold energy. The kinetic shift contributes to the slow rise in the SDIE curve of ions produced by further fragmentation. The slow rise near threshold in the SDIE curves of IV and VI indicate that the kinetic shift is relatively greater for the decompositions forming IV and VI than for decompositions forming III and V.

The SDIE curve of III shows a maximum at 9.45 eV, which is in good agreement with the value of 9.22±0.30 eV calculated for a one bond

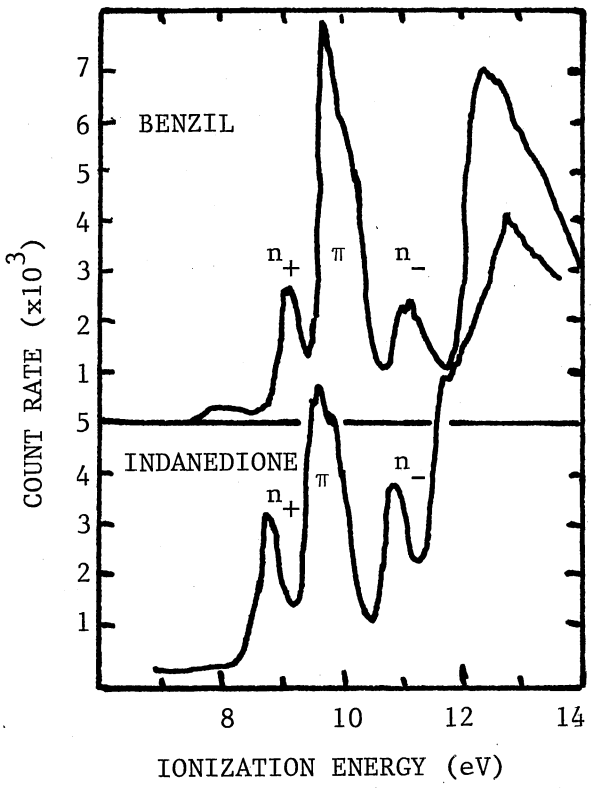

Figure 17. Photoelectron Spectrum of Benzil

rupture mechanism (Scheme I). The calculated appearance potential 10.04±0.30 eV for IV, also assuming one bond rupture of the molecular ion, is compariable to 10.35 eV, a local maximum in the SDIE curve of IV.

The agreement between calculated and experimental appearance potentials for III and IV, and the slopes in the SDIE curves of these ions indicate that the molecular ion (II) competitively dissociates by rupture of the central carbon carbon bond to form IV and the benzoyl-$\underline{d}_5$ radical of IV and the 4-methoxybenzoyl radical.

Energy Deposition

The energy deposition function of the molecular ion is computed from the SDIE curves of all ions formed (N) and the factor (V-E) (Equation 3).[23]

$$P(ED)_{Ei,V} = \sum_{J=I}^{N} SDIE\ (J)_{Ei} \times (V-E) \qquad (3)$$

The SDIE $(J)_{Ei}$ term represents the value of the SDIE curve of the $J^{\underline{th}}$ ion at an internal energy Ei, V is the total ionizing beam energy, and E is the total energy (ionizion plus internal) of the ions. The factor (V-E) must be included to obtain the correct transition probabilities applicable to a certain ionizing beam energy. For ionizing beam energies greater than 10-15 eV above the ionization potential the term (V-E) is essentially constant and was omitted.

An estimate of the 70, 20.6, 15.19, and 13.39 eV P(ED) function of the molecular ion of I was obtained (Equation 4).

$$P(ED)_{Ei,V} \simeq \sum_{J=I}^{VII} SDIE\ (J)_{Ei} \times (V-E) \qquad (4)$$

The 70 eV P(ED) function is reproduced in Figure 18, calculated from Equation 4 without the (V-E) factor. This P(ED) function has the same form and energy spread as those obtained for 4-methylbenzil and 4-methoxybenzil.

Variations in transition probabilities with the ionizing beam energy are illustrated in Figure 19. The curves are energy deposition functions applicable to 13.39, 15.19, and 20.6 eV mass spectra of I. These low energy P(ED) functions are normalized to unit area.

Breakdown Graph

The breakdown graph obtained from the SDIE curve of each ion normalized by their sum at each value of the internal energy of the molecular ion is reproduced in Figure 20. For identification a few points are included on each curve. The stability of the molecular ion (II) decreases rapidly with internal energy of more than one electron volt. The 4-methoxybenzoyl ion (III) dominates the stable ions formed from molecular ions with up to 6.5 eV of internal energy. At most, the stable benzoyl-$\underline{d}_5$ ion (IV) is only 20.4% of the stable ions formed at any given internal energy. In the study, VI is the only stable ion observed above 12.00 eV of internal energy.

Relative Rate

The ratio of relative rates for the fragmentation of II as a function of the electron energy minus the ionization potential (internal energy) of II is given in Equation 5.

$$\frac{k_2(E)}{k_1(E)} = \frac{\text{SDIE (IV)}_{Ei} + \text{SDIE (VI)}_{Ei}}{\text{SDIE (III)}_{Ei} + \text{SDIE (V)}_{Ei} + \text{SDIE (VII)}_{Ei}} \qquad (5)$$

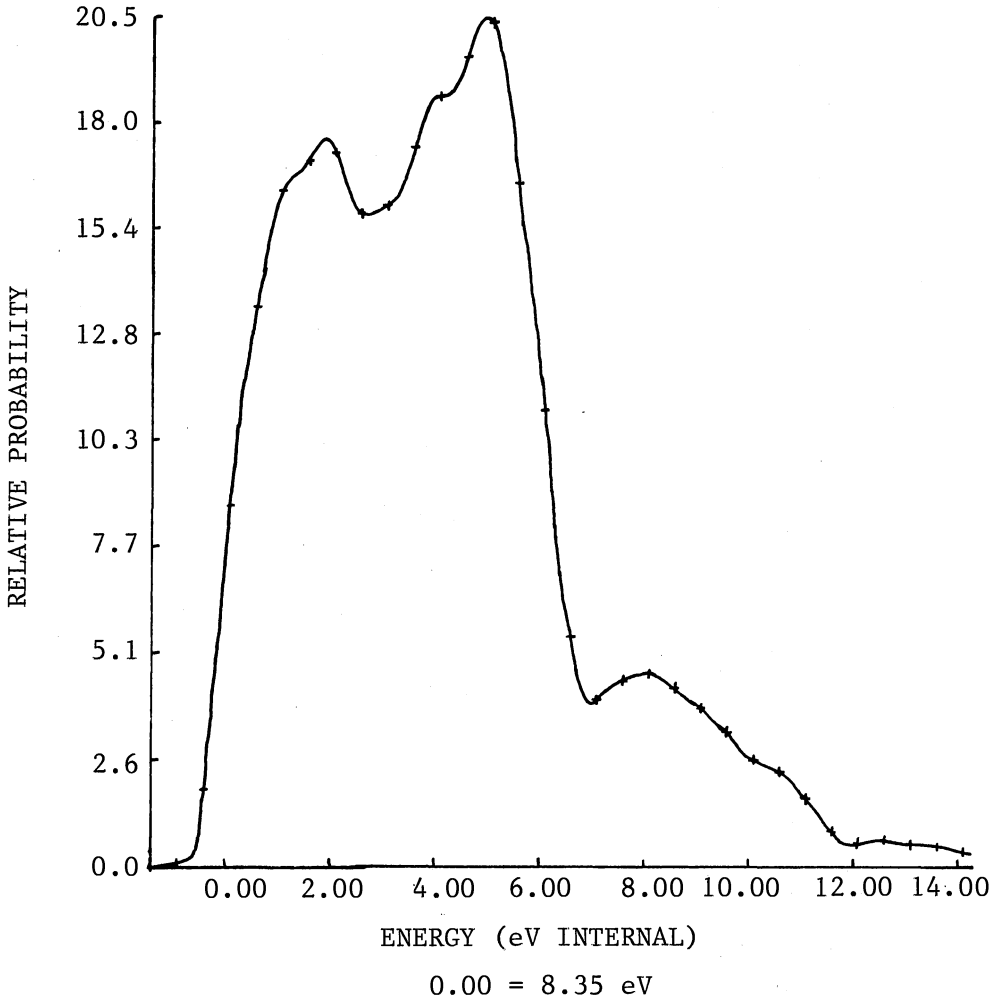

Figure 18. Energy Deposition Function for the Molecular Ion of I (II) at 70 eV

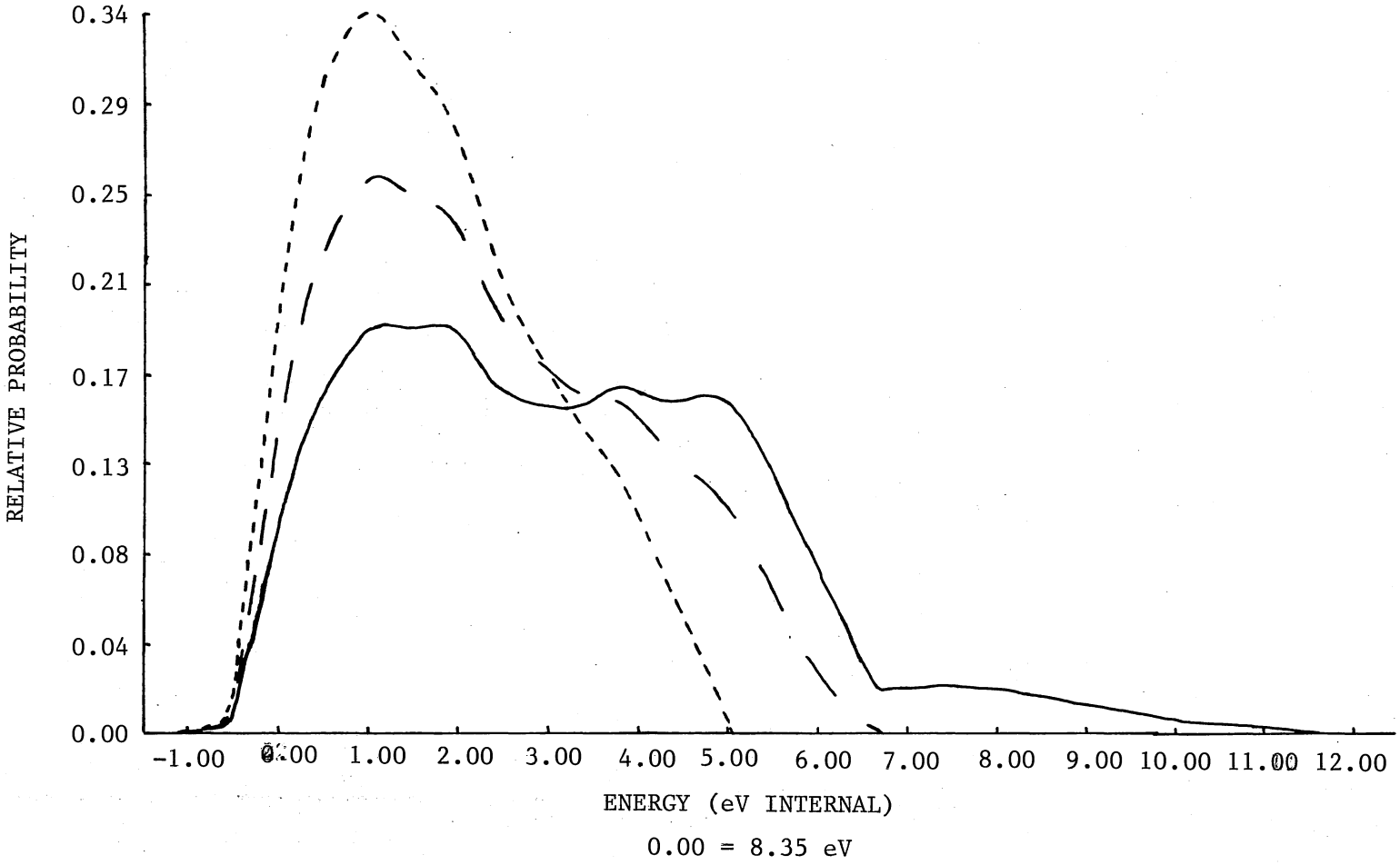

Figure 19. Deposition Functions for II applicable to Low Ionizing Voltages

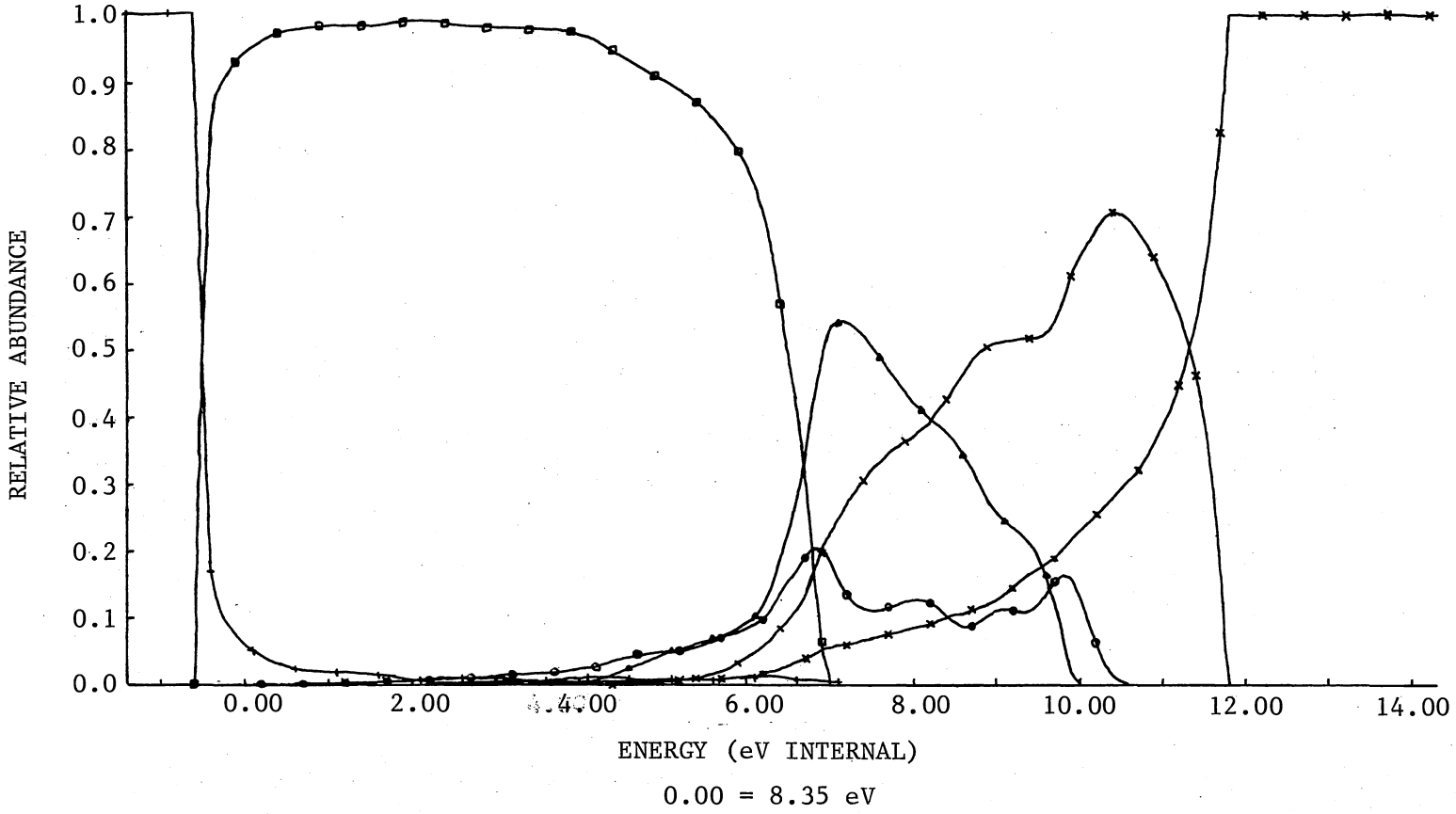

Figure 20. Breakdown Graph of 4-Methoxybenzil-$\underline{d}_5$

The ratio was calculated at 0.1 eV intervals. A curve drawn through these values is presented in Figure 21. The graph is the average of two sets of data obtained for each ion. The rate constant, $k_1(E)$, for the formation of III is greatly dominant to an internal energy of 6.0 eV. At this internal energy the high energy process, formation of IV, becomes more significant and increases rapidly. The peak at 7.00 eV may be an artifact caused by the uncertainty in determining the change in the gradient of the FDIE curve for III in the region of its maximum. Within experimental error, energy randomization of the molecular ion appears to be essentially complete up to an internal energy of $\sim$8.0 eV. However, large error limits at internal energies of $\sim$7.0-9.0 eV make conclusions about energy randomization in this region tenous.

Comparison of Ion Intensities

Table IV lists calculated and experimental ion intensities normalized to 100 for III. Calculated ion intensities may be obtained from double integration of the SDIE curves or single integration of the FDIE curves to the same energy as the electron beam, or from the appropriate energy deposition function folded into the breakdown graph. In practice Equation 16 (Appendix D) was used for calculating ion intensities by the last method. In the low energy mass spectra, the calculated relative abundances agree well with the experimental values. The ion intensities in the 70 eV mass spectrum correlates well with the exception of ions IV and VI, which are formed by the higher energy process. The reasonable comparison of ion intensities for the 70 eV mass spectrum indicate that the ionization efficiency curve of each ion has become flat. Table V gives the average relative slope in the region to

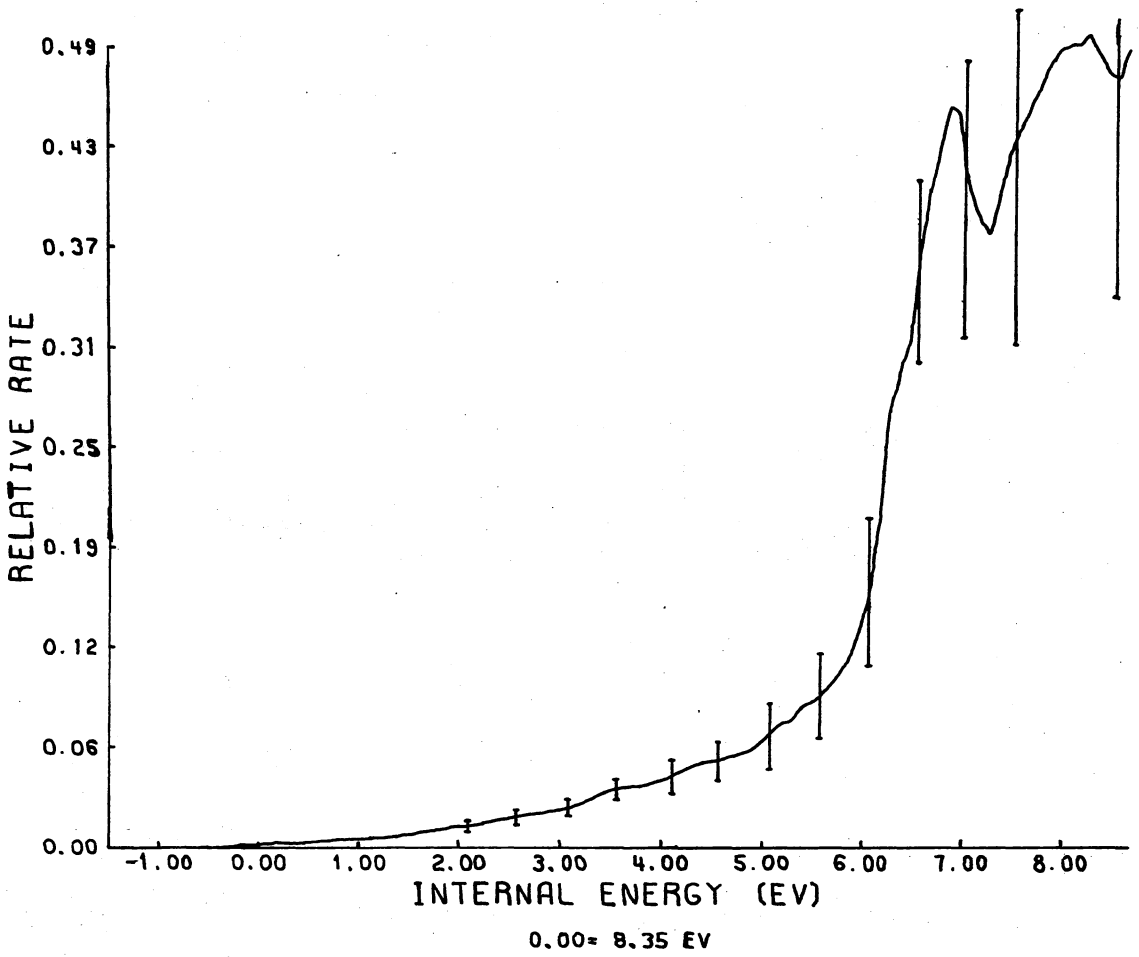

Figure 21. Relative Rate Constant Plot of 4-Methoxybenzil-$\underline{d}_5$

TABLE IV

CALCULATED AND EXPERIMENTAL ION INTENSITIES
OF 4-METHOXYBENZIL-$\underline{d}_5$

Ion	13.39 eV			15.19 eV			18.09 eV		
m/e	Meas.	Calc.[a]	Calc.[b]	Meas.	Calc.[a]	Calc.[b]	Meas.	Calc.[a]	Calc.[b]
245	1.6	1.9	1.3	1.4	1.5	1.1	1.2	1.3	1.0
135	100.0	100.0	100.0	100.0	100.0	100.0	100.0	100.0	100.0
110	0.9	0.7	0.7	1.8	1.5	1.5	3.2	2.5	2.6
107	0.2	0.1	0.1	1.2	0.7	0.7	3.9	2.7	2.8
82				0.1	0.1	0.1	0.5	0.4	0.4
77				0.1	0.1	0.1	2.0	1.4	1.4

m/e	20.6 eV			70 eV		
245	1.2	1.1[a]	1.0[b]	1.2	1.1[c]	0.9[b]
135	100.0	100.0	100.0	100.0	100.0	100.0
110	4.2	3.2	3.2	7.3	4.7	4.5
107	5.7	3.9	4.0	8.3	7.1	6.7
82	1.4	0.9	0.9	9.4	4.4	3.6
77	4.5	3.1	3.1	10.8	8.1	7.3

[a]Double Integration of SDIE [b]Equation 16 [c]Single Integration of SDIE

TABLE V

FALL IN FDIE CURVE FOR EACH ION FORMED FROM I

Ion m/e	Slope	Normalized Slope[a]
245	-60±40	-11±7
135	-6400±800	-12±1.5
110	-250±30	-10±1.5
107	-440±70	-12±2
82	-180±80	-8±3.5
77	-390±80	-9±2

[a]Normalized to 100 for the maximum in each curve

the right of the maximum in each FDIE curve. The slope for each ion is within experimental error. The fall in the FDIE curves indicate that the ionization cross section for electron impact of I is nearing a maximum. Examination of the FDIE curves of IV, VI, and VII reveals localized changes in these slopes. This suggests that although I may be nearing a maximum in its ionization cross section, there are transitions from the molecule that lead to stable IV, VI, and VII. This produces positive peaks in the derivative of the total FDIE curve of these ions. A comparison of the relative area under the SDIE curves to the area under the positive peaks plus the area under the SDIE curves is tabulated in Table VI. The relative abundances of IV and VI increase 2% and 4.5%, respectively. Although these contributions to the relative abundances are small, they are only for a 3-4 eV range. This indicates that there are transitions of the molecule that lead to stable ions that have not been taken into account. This is one reason for the discrepancy of the calculated and experimental ion intensities of IV and VI. Therefore, only semi-quantitative features of the 70 eV mass spectrum may then be obtained from a knowledge of the processes occuring from the ionization potential of the molecule to $\sim$20 eV of internal energy.

Benzil

Fragmentation Scheme

The 70 eV mass spectrum of benzil is given in Figure 22.[18] The contribution of four ions, m/e 210, 105, 77 and 51, to the total percent ionization is given in Table VII. The mass spectrum of benzil at

TABLE VI

COMPARISON OF RELATIVE AREA UNDER
SDIE AND TOTAL d^2I/dE^2 CURVES

Ion m/e	SDIE	Total d^2I/dE^2
245	1.1	1.1
135	100.0	100.0
110	4.7	4.8
107	7.1	7.1
82	4.4	4.6
77	8.1	8.2

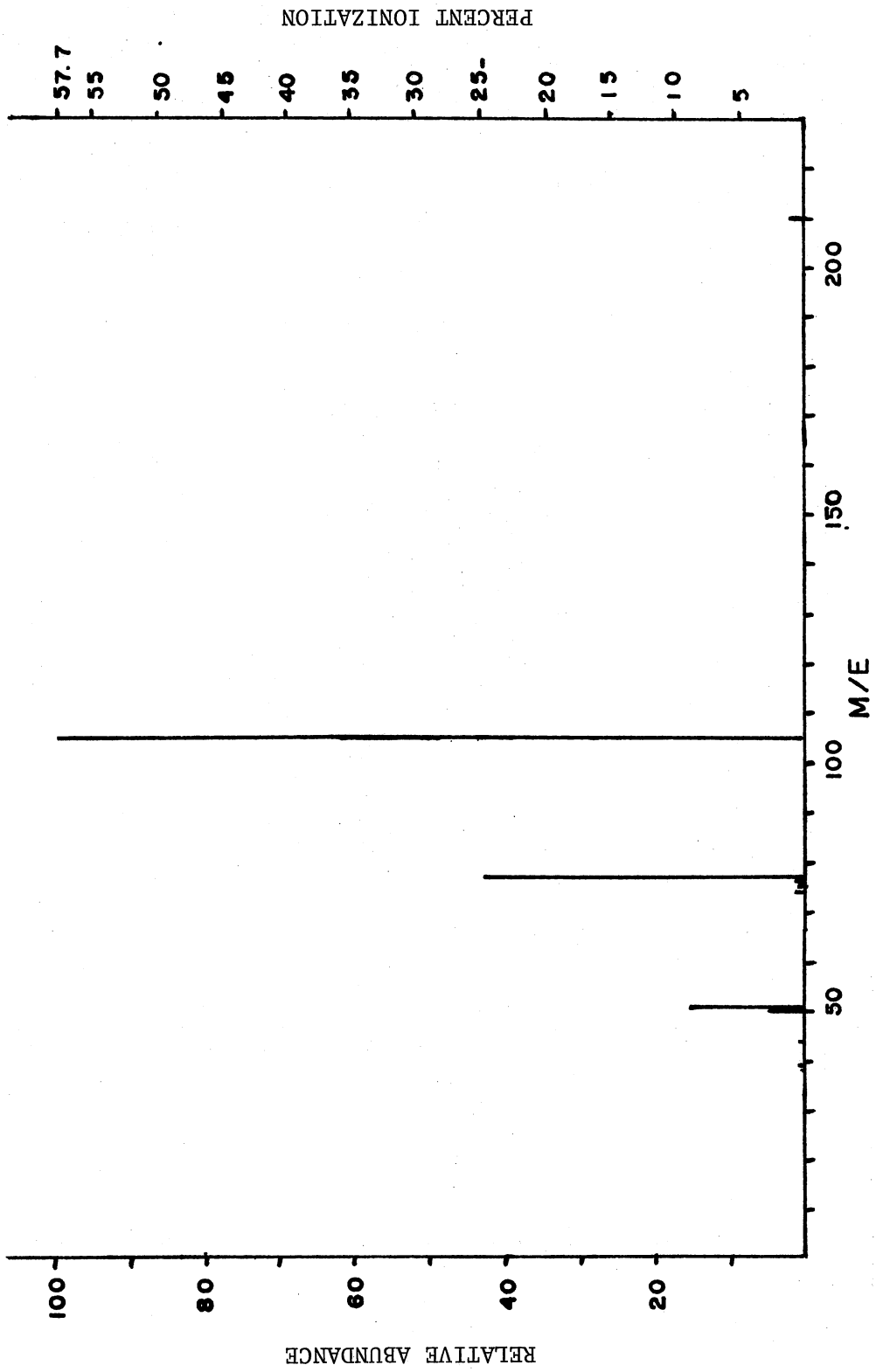

Figure 22. 70 eV Mass Spectrum of Benzil

TABLE VII

ION ABUNDANCES OF BENZIL

	m/e				
eV	210	105	77	51	Total
14.55	2.5	96.0	1.4	0.1	100.0%
15.95	2.2	93.7	4.0	0.1	100.0%
20	1.6	82.5	14.0	0.2	98.3%
70	1.1	58.0	24.7	8.9	92.7%

70 eV is dominated by these ions and consists completely of these ions below 20 eV.

A fragmentation pattern, based upon conclusions drawn from the study of 4-methyl and 4-methoxy homologues is given in Scheme II (Figure 23). The molecular ion formed by the electron impact on benzil fragments to form the benzoyl ion, m/e 105, and the benzoyl radical. The benzoyl ion looses carbon monoxide to form the m/e 77 ion, which may further decompose to form the m/e 51 ion by the loss of ethylene.

Derivatives of Ionization Efficiency

The FDIE curves and experimental dI/dE values for these ions are reproduced in Figures 24-27. All ions are normalized to the maximum of the most intense ion (m/e 105) which was given a value of 100.

The SDIE curves are given in Figures 28-31. The SDIE curve of the molecular ion gives an ionization potential for benzil of 8.65 eV. The reported ionization potential of benzil is 8.78±0.20 eV.[19] The curve also reveals high lying electronic states of the ion and/or autoionization levels for the molecule. Such peaks have been observed for 4-methoxybenzil-d_5, 4-methoxybenzil, and in the pes spectrum of benzil. The SDIE curve for the benzoyl ion, m/e 105, gives an appearance potential of 9.65 eV. This is in very good agreement with a reported value of 9.70±0.20 eV.[19] From Figure 30, the appearance potential of m/e 77 is $\leq$ 15.45 eV. A experimental value was previously reported at 15.12± 0.20 eV.[19] Due to the weak signal for the m/e 51 ion, its SDIE curve was difficult to obtain. In Figure 31, the data below 7.70 eV is due to instrumental noise and/or background. A calculated appearance potential is 15.36±0.70 eV (See Appendix A).

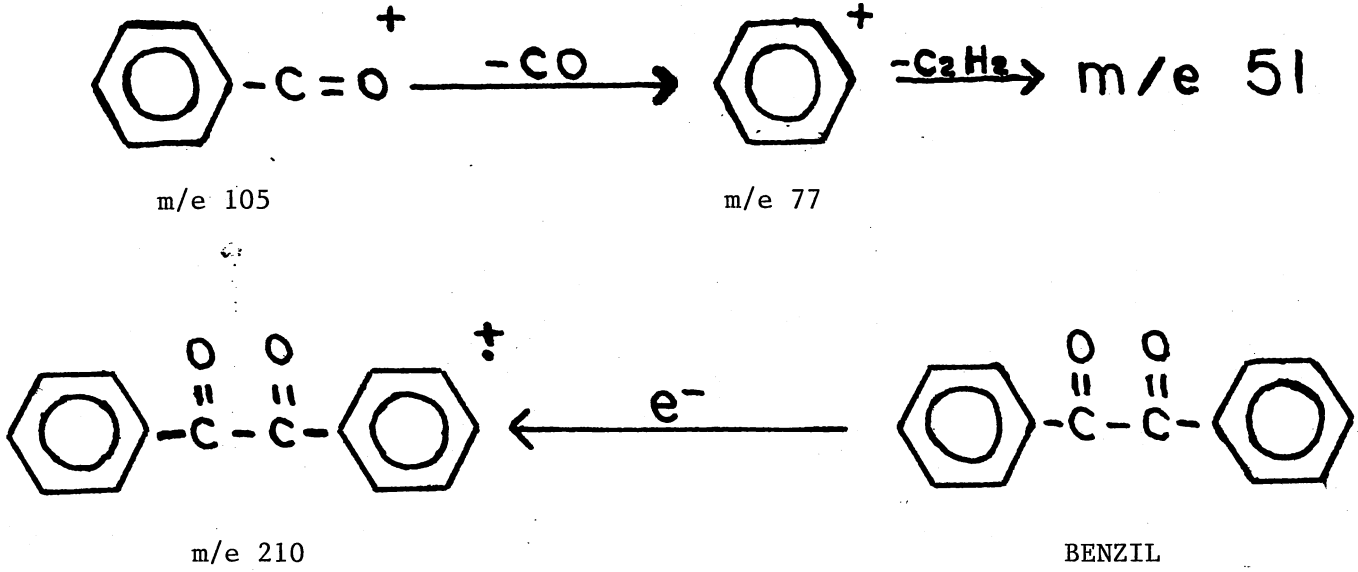

Figure 23. Scheme II. Detailed Fragmentation for Benzil

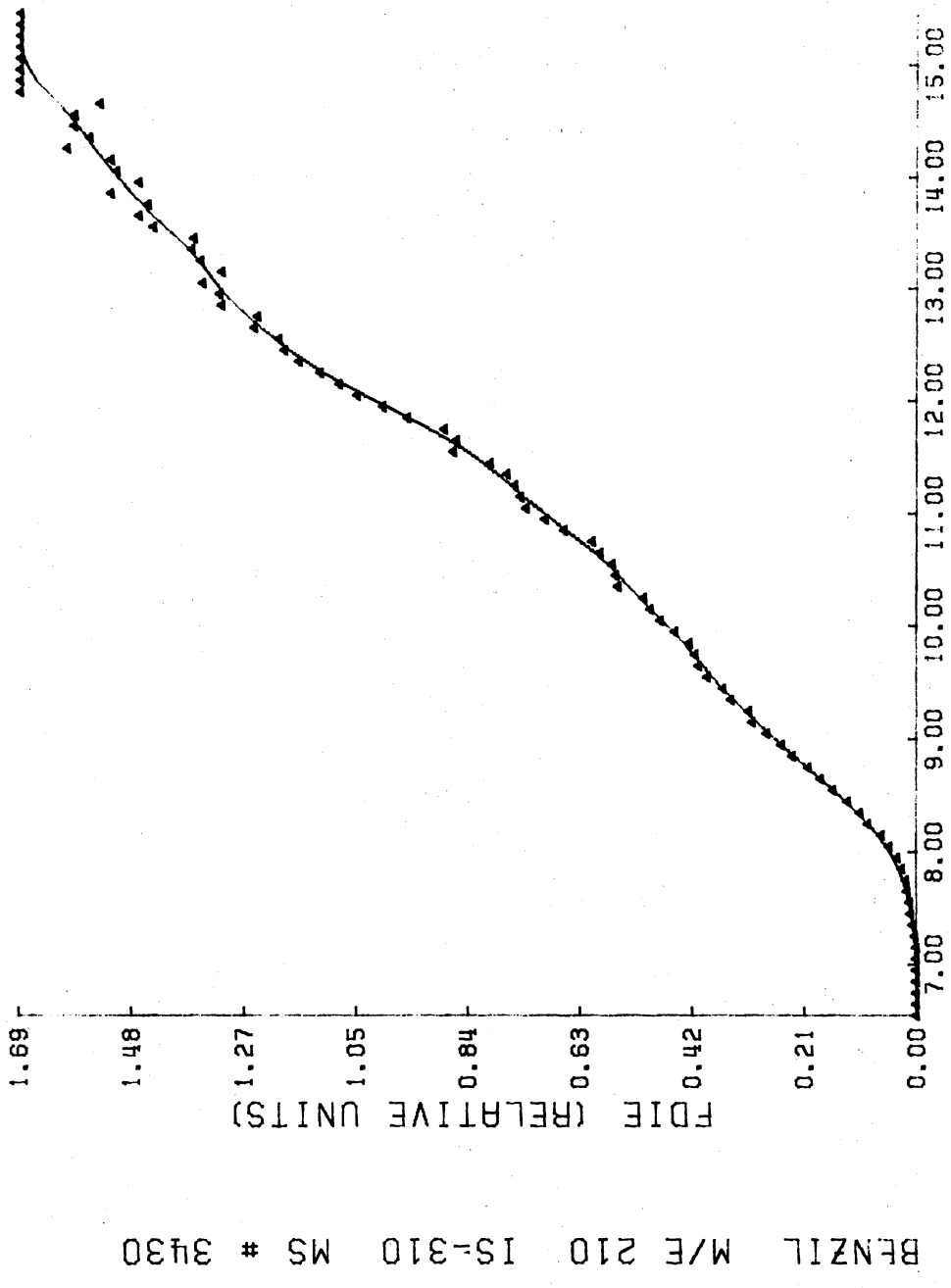

Figure 24. FDIE Curve of m/e 210

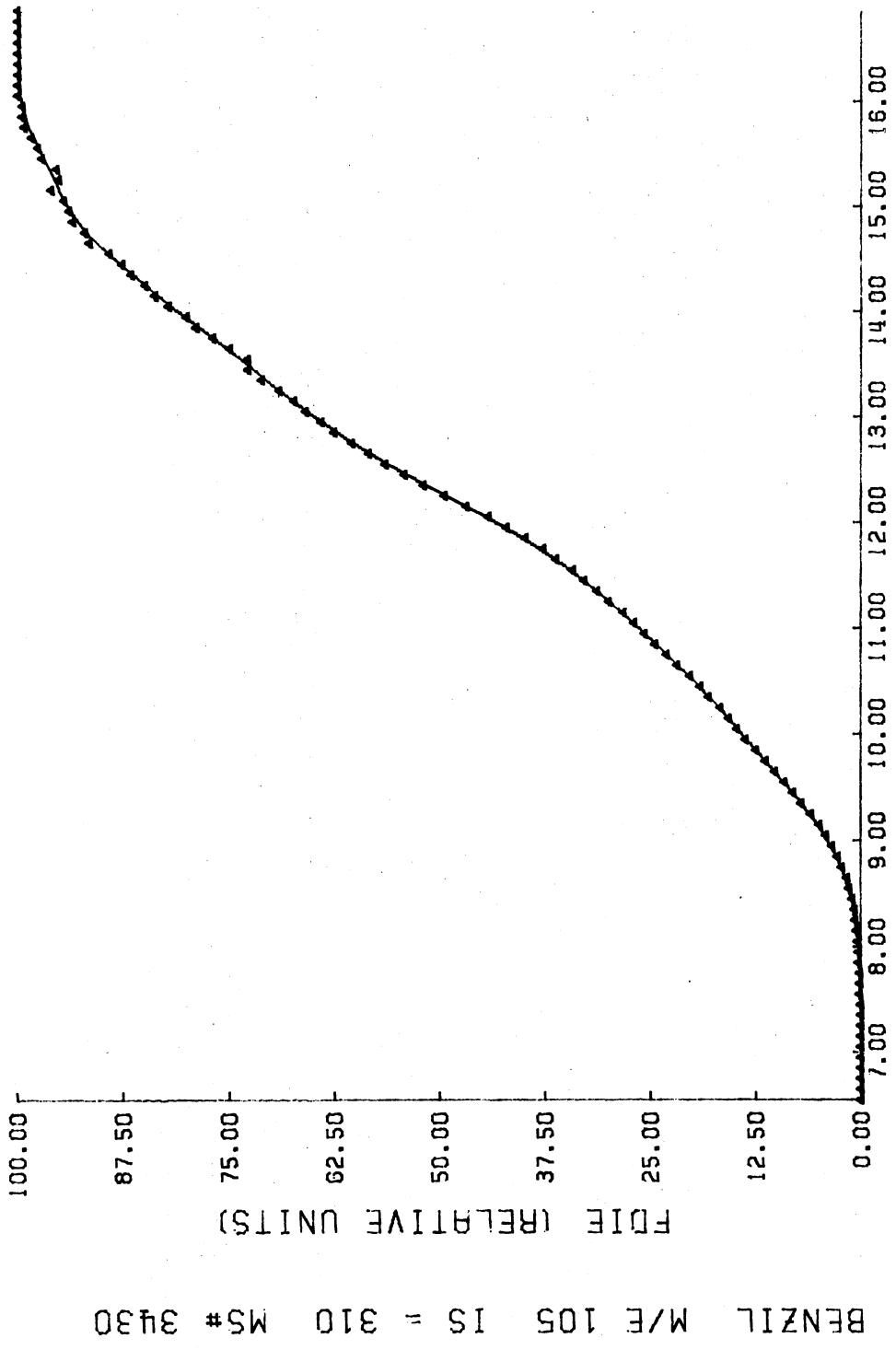

Figure 25. FDIE Curve of m/e 105

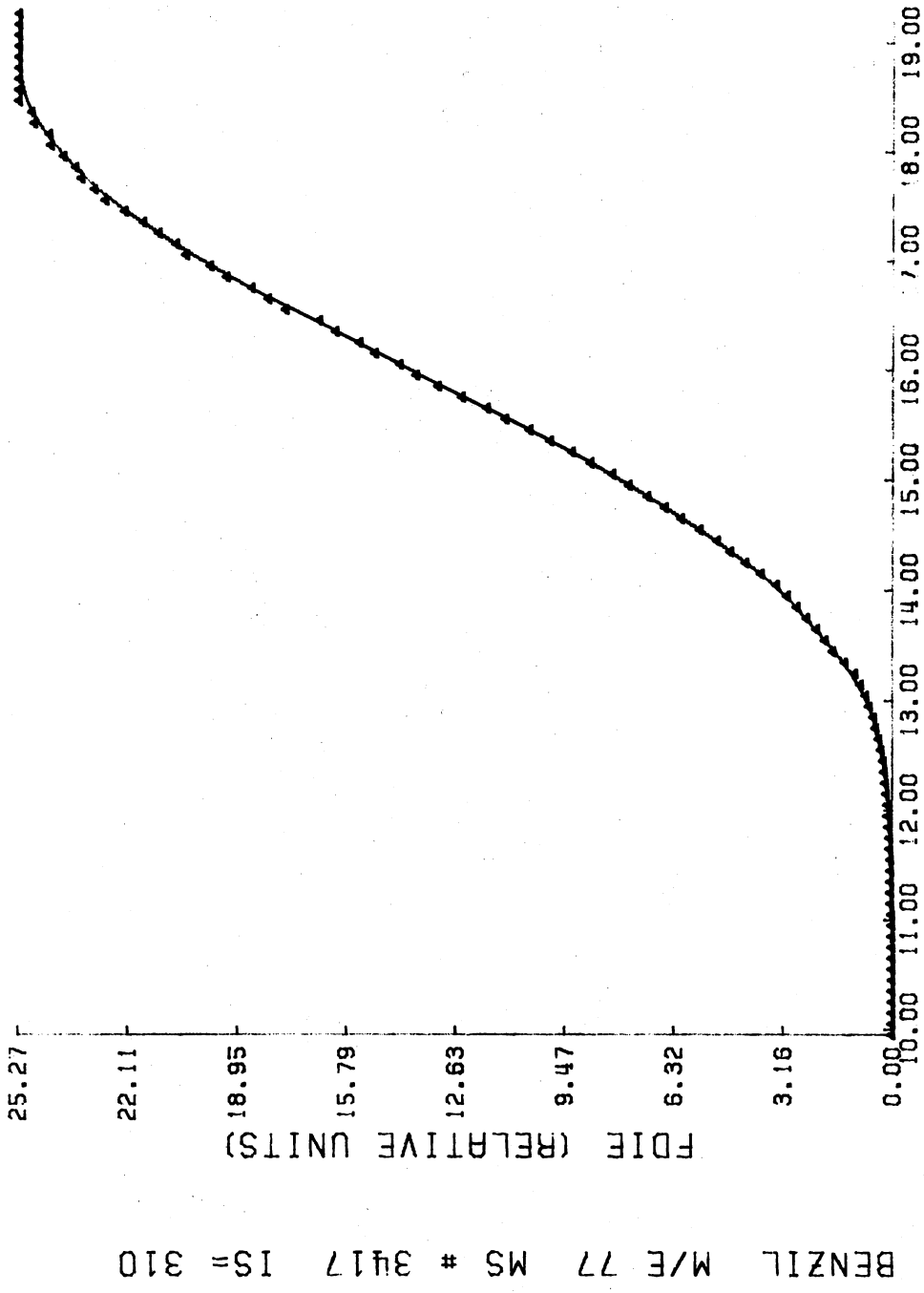

Figure 26. FDIE Curve of m/e 77

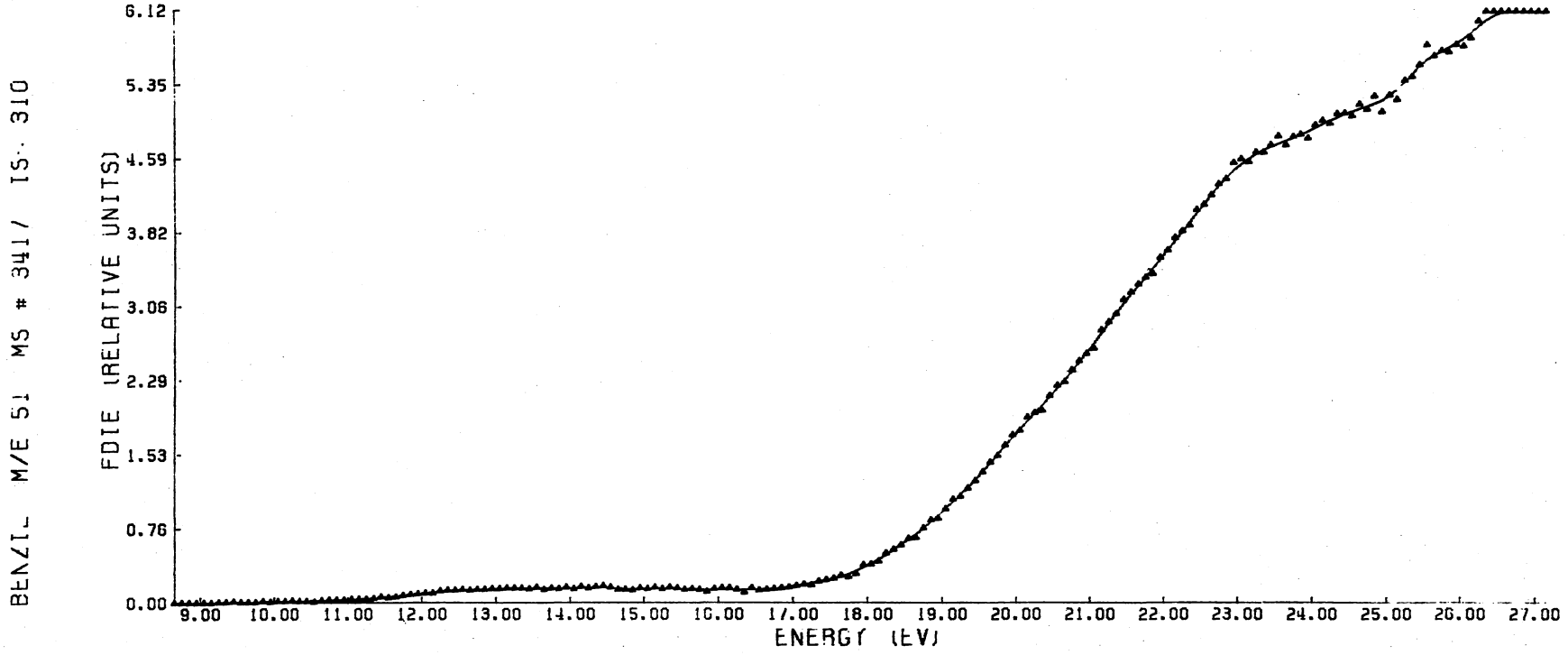

Figure 27. FDIE Curve of m/e 51

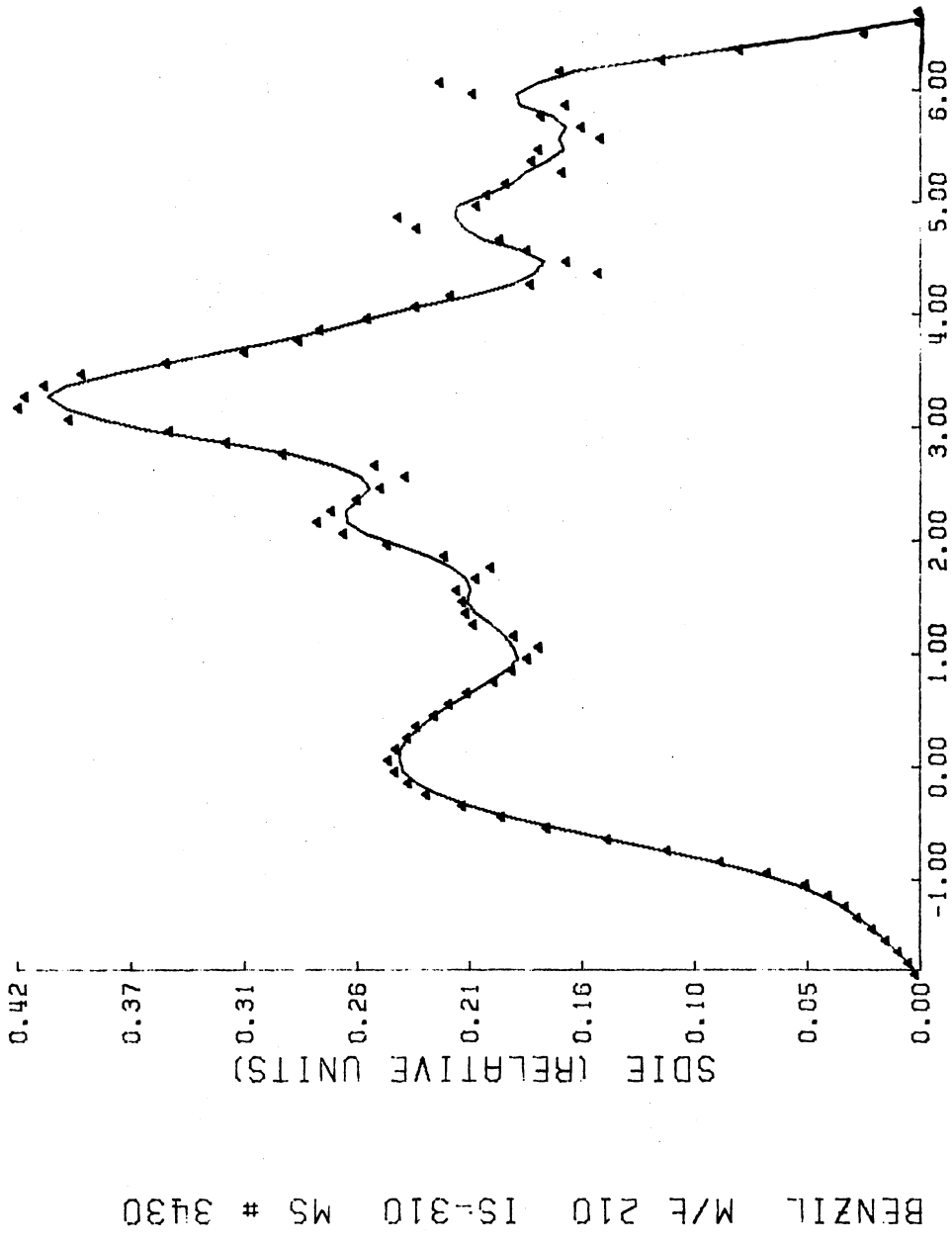

Figure 28. SDIE Curve of m/e 210

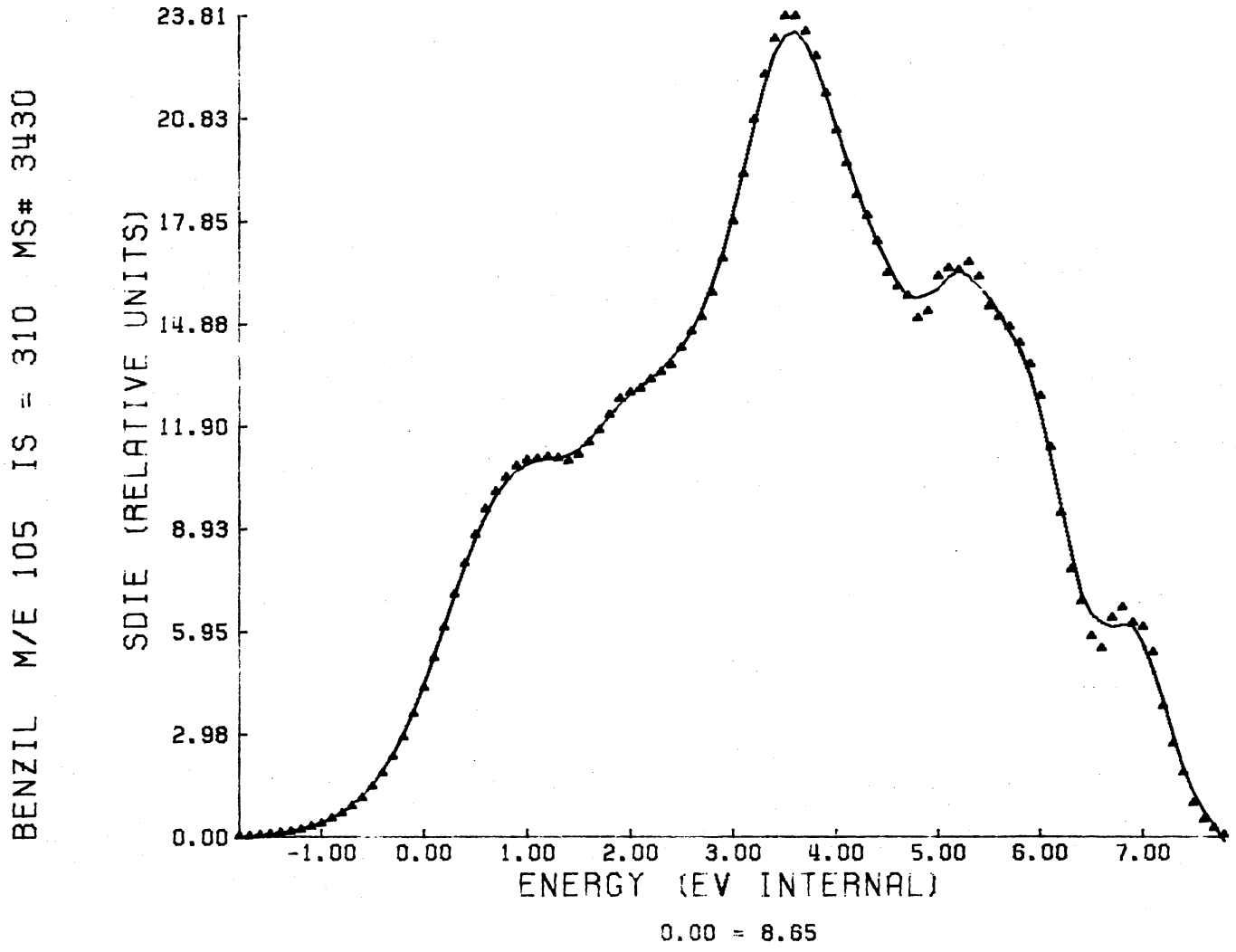

Figure 29. SDIE Curve of m/e 105

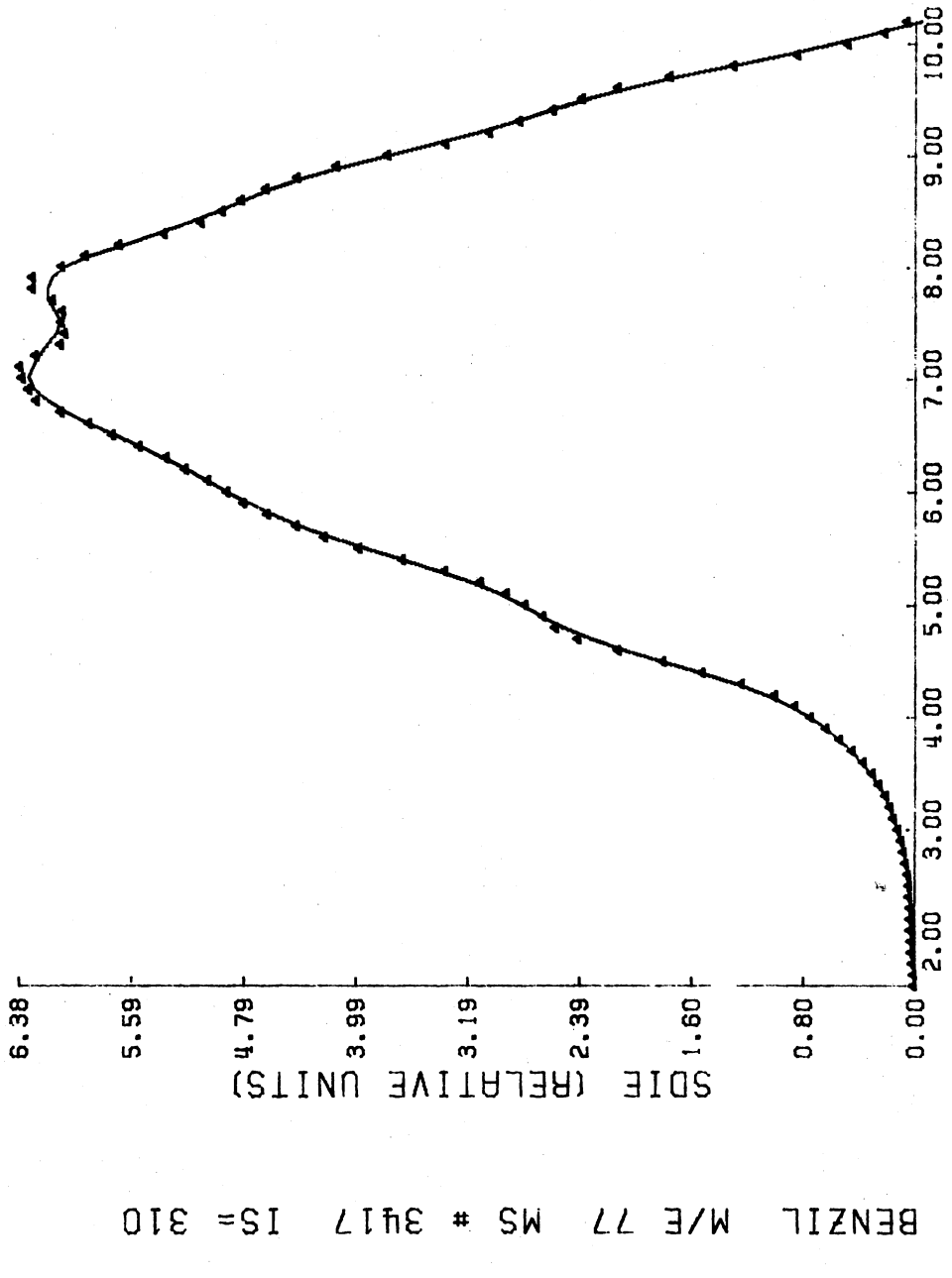

Figure 30. SDIE Curve of m/e 77

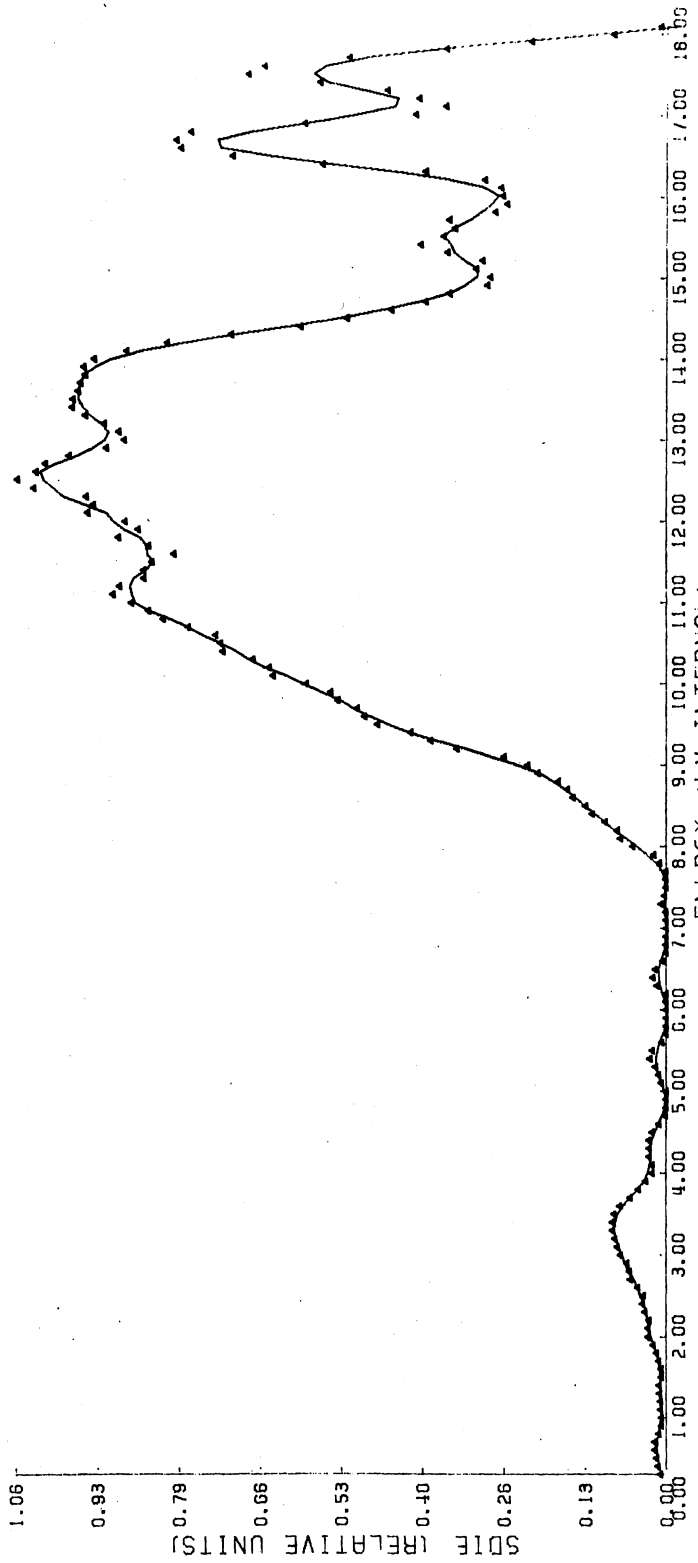

Figure 31. SDIE Curve of m/e 51

The theoretical standard deviation of the FDIE data, the resulting standard deviation calculated for SDIE, and the experimental multiplier gain for each ion at three electron energies is given in Table VIII. As observed for the 4-methyl and 4-methoxy (Table III) compounds, the multiplier gain is slightly mass discriminate which appears to be an indirect function of the ionizing beam energy.

Energy Deposition

The energy deposition function obtained for benzil at an ion source temperature of 310° C is given in Figure 32a. The curve extends over the same range as the P(ED) functions obtained for 4-methylbenzil and 4-methoxybenzil-$\underline{d}_5$. The percent contribution made by the ions is given in Table IX. Also in this table is a comparison of ions with m/e 210, 105, and 77 produced from benzil at an ion source temperature of 250° C[24] and 310° C. The energy deposition function obtained for benzil-$\underline{d}_5$ is given in Figure 32b.[11] The total area under these P(ED) functions in Figure 32 is 127.06 (minus the contribution from m/e 51) for benzil (I.S.= 310° C) and 127.20 for benzil-$\underline{d}_5$ (I.S.= 250° C). The ratio is 0.99±0.01. The extent of ionization of these molecules remains the same, but increased thermal energy decreases the contribution of the molecular ion and increases the relative contribution of the m/e 77 (m/e 82) ion.

Breakdown Graph

The breakdown graph for benzil is given in Figure 33. It can be seen that the relative amount of stable molecular ions decreases rapidly with energy in excess of the ionization potential. The graph

TABLE VIII

PERCENT STANDARD DEVIATION AND
MULTIPLIER GAIN FOR BENZIL

Ion m/e	eV[a]	%σFDIE[b]	%σSDIE	Gain ($\times 10^{-4}$)
210	8.05	5.62	5.57	2.59
	9.15	3.31	7.57	1.75
	13.95	3.32	32.12	2.04
105	9.15	1.14	5.06	2.42
	11.35	0.72	5.32	1.96
	15.65	0.72	14.98	2.00
77	12.85	3.88	5.52	0.90
	15.45	0.90	5.35	1.02
	17.45	0.92	7.56	1.08
51	12.05	7.70	12.15	1.35
	20.85	2.05	8.35	1.18
	26.25	2.15	24.45	1.39

[a] Corrected

[b] For each ion the lock-in-amplifier time constant (sec.), and integration time (sec.) are: m/e 210,30,1; m/e 105,10,1; m/e 77,10,1; m/e 51,30,1. The sampling interval was 11 seconds.

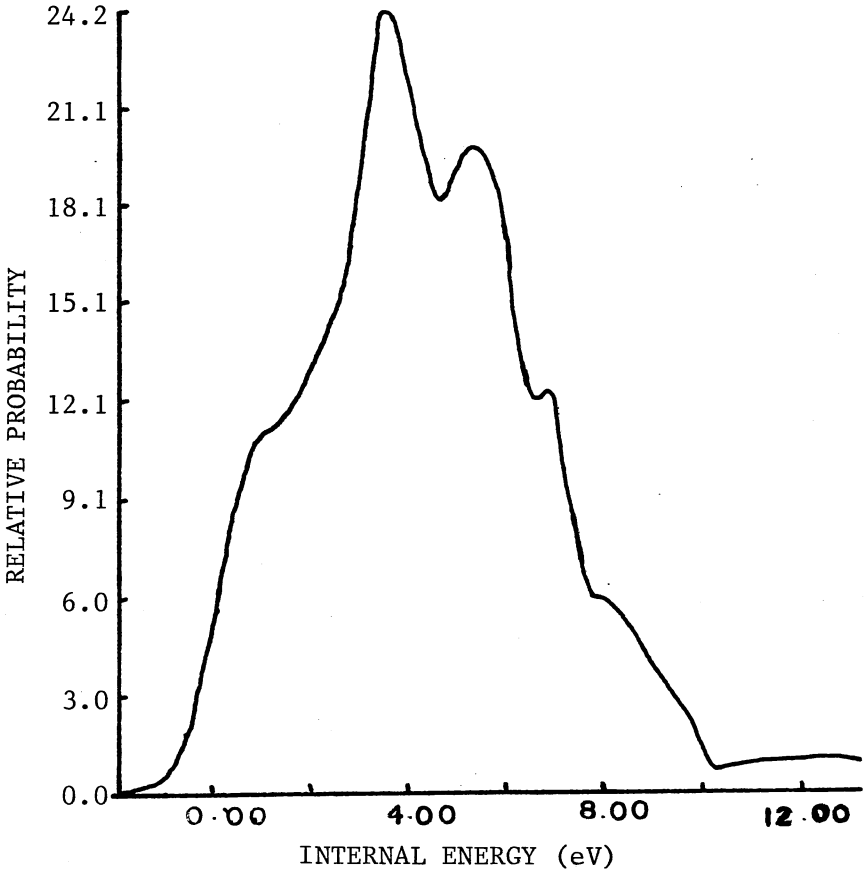

Figure 32a. Energy Deposition Function for Benzil at I.S. = 310° C

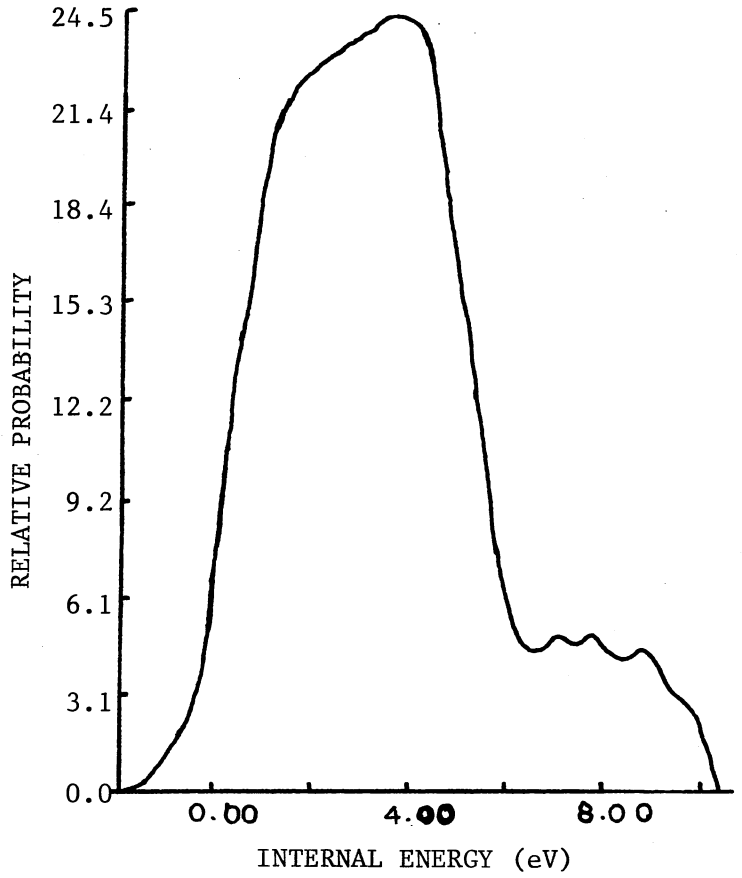

Figure 32b. Energy Deposition Function for Benzil-d_5 at I.S. = 250° C

TABLE IX

PERCENT CONTRIBUTION TO AREA
UNDER P(ED) FOR BENZIL

Ion m/e	% P(ED)	% P(ED)[a]	% P(ED)[b]
210	1.3	2.9	1.4
105	75.1	78.6	78.7
77	19.0	18.5	19.9
51	4.6		

[a]For Benzil at 250° C, Reference 24

[b]For ions m/e 210, 105, and 77 only

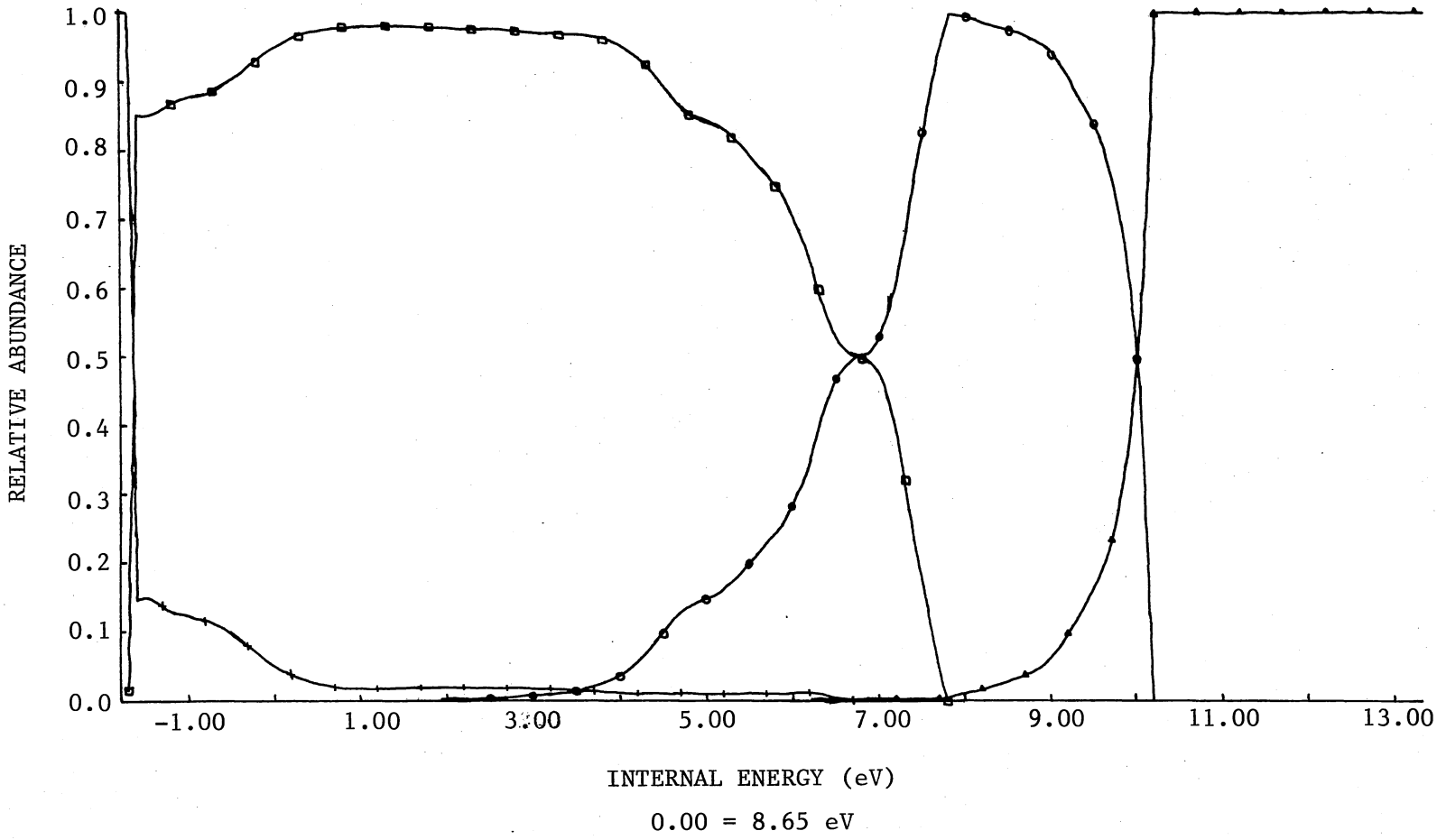

Figure 33. Breakdown Graph for Benzil

is dominated by the benzoyl ion at low internal energies of the molecular ion. Above 10.5 eV no stable m/e 210, 105, or 77 ions were observed.

Ion Intensities

Comparison of calculated and experimental mass spectra of benzil is given in Table X. The comparison of low energy mass spectra is very good. The 70 eV mass spectra is in poor correlation for ions with m/e 77 and 51. Analogous reasons for this discrepancy could be made as those for the comparison of experimental and calculated ion intensities of 4-methoxybenzil-$\underline{d}_5$.

TABLE X

EXPERIMENTAL AND CALCULATED ION INTENSITIES OF BENZIL

14.55 eV				15.95 eV			
Ion m/e	Meas.	Calc.[a]	Calc.[b]	Ion m/e	Meas.	Calc.[a]	Calc.[b]
210	2.6	2.3	1.9	210	1.9	2.0extp.	1.8
105	100.0	100.0	100.0	105	100.0	100.0	100.0
77	1.5	2.0	2.1	77	4.2	4.8	5.0
51	0.2	0.2	0.2	51	0.1	0.2	0.2
20 eV				70 eV			
Ion m/e	Meas.	Calc.[a]	Calc.[b]	Ion m/e	Meas.	Calc.[c]	Calc.[b]
210	2.1		1.7	210	1.9	1.7	1.6
105	100.0		100.0	105	100.0	100.0	100.0
77	16.8	16.8expt.	14.3	77	43.0	25.3	24.2
51	0.3	0.6	0.4	51	15.9	6.1	3.2

[a]Double Integration of SDIE

[b]Equation 16

[c]Single Integration of SDIE

CHAPTER III

EXPERIMENTAL

4-Methoxybenzil-d5 (I)[25]

Benzene-$\underline{d}_6$ (Merck, Sharp, and Dohme) was brominated and the Grignard made. Bis(phenyl-$\underline{d}_5$) cadmium[26,27] was obtained from the benene-$\underline{d}_5$ magnesium bromide and cadmium chloride. 4-Methoxyphenylacetic acid was converted to the acid chloride with sulfonyl chloride.[28] 4-Methoxybenzyl phenyl-$\underline{d}_5$ ketone was prepared from bis(phenyl-$\underline{d}_5$) cadmium and 4-methoxyphenylacetyl chloride, which was then oxidized with selenium dioxide to 4-methoxybenzil-$\underline{d}_5$ (I).[29] Crude I was recrystallized twice from methanol, m.p. 62.0-62.2° C.

4-Methoxybenzil[30]

4-Anisyl benzyl ketone (Aldrich) was oxidized to 4-methoxybenzil with selenium dioxide.[29] Recrystallization from carbon tetrachloride yielded 4-methoxybenzil, m.p. 62.0-62.7° C. (lit. 61-62° C).[31]

Benzil

Benzil (Eastman Kodak) was used without further purification.

Instrumentation[11]

Mass spectra and the first derivatives of the ionization

efficiency were determined with an LKB 9000P mass spectrometer.[32] Xenon was introduced into the ion source via the direct probe, which was modified for gas inlet. To maintain uniform sample pressure, the compounds were introduced into the ion source through the gas chromatograph inlet system. The oven temperature was 153° C, separators 160° C, and ion source 250° C for studies of 4-methoxybenzil-$\underline{d}_5$. The oven temperature was 125° C, separators 150° C, and ion source 310° C for studies of benzil. The trap was maintained constant at 20 μA, and the electron shield was zero potential with respect to the filament. The extraction plates were set near the block potential except for 70 eV mass spectra. To insure flat-topped peaks and maximize the ion intensity the exit and collector slits were at 0.10 and 0.75 mm, respectively. The dI/dE data was read from a General Radio Corp. Electronic Counter Type 1151-A; and in electron energy steps of 0.100±0.003 eV to the maximum and then for ions formed from 4-methoxybenzil-$\underline{d}_5$ in steps of 0.300±0.003 eV for 3-4 eV further. All other instrumental conditions were the same as previously reported.[8,11,33]

Numerical Treatment

The dI/dE data for each ion, except Xenon, was smoothed twice using subroutine SE-15[34] and the result was taken to be the first derivative of the ionization efficiency curve, FDIE. The FDIE curve for each ion was numerically differentiated[35] to obtain d^2I/dE^2; the values were smoothed once to obtain the second derivative curve, SDIE.

The standard deviation (σ_{true}) in the dI/dE data has been theoretically computed from considerations of the electron multiplier noise, absolute ion intensity, lock-in-amplifier time constant, and

integration time of the frequency counter (See Apendix B).[36]

BIBLIOGRAPHY

1. H. M. Rosenstock, M. B. Wallenstein, A. L. Wahrhaftig, and H. Eyring, Proc. Natl. Acad. Sci. U.S. 38, 667 (1952).

2. For reviews see: a) H. M. Rosenstock and M. Krauss, "Mass Spectrometry Of Organic Ions", F. W. McLafferty, Ed., Academic Press, New York, N. Y., 1963, Chapter 1; b) H. M. Rosenstock, Advan. Mass Spectrom. 4, 523 (1968).

3. a) J. D. Morrison, J. Chem. Phys. 21, 1767 (1953); b) J. D. Morrison, Rev. Pure Appl. Chem. 5, 22 (1955).

4. W. A. Chupka, J. Chem. Phys. 30, 191 (1959).

5. E. Petterson and E. Lindholm, Ark. Fys. 24, 49 (1963).

6. R. Stockbauer, J. Chem. Phys. 58, 3800 (1973).

7. G. G. Meisels, C. T. Chen, B. G. Giessner, and R. H. Emmel, J. Chem. Phys. 56, 793 (1972).

8. S. E. Scheppele, R. K. Mitchum, K. F. Kinneberg, G. G. Meisels, and R. H. Emmel, J. Amer. Chem. Soc. 95, 5105 (1973).

9. a) M. L. Vestal, J. Chem. Phys. 43, 1356 (1965); b) M. L. Vestal, "Fundamental Processes in Radiation Chemistry", P. Ausloss, Ed., Interscience, New York, N. Y., 1968, Chapter 2.

10. M. S. Chin and A. G. Harrison, J. Mass Spectrom. 2, 1073 (1969).

11. R. K. Mitchum, Ph. D. Thesis, Oklahoma State University, Stillwater, Ok., 1973.

12. C. E. Moore, Nat. Bur. Stds. (U.S.), Circ. 467 (1952).

13. R. E. Huffman, Y. Tanaka, and J. C. Larrabee, J. Chem. Phys. 39, 902 (1963).

14. P. Marmet, E. Bolduc, and J. J. Quemener, J. Chem. Phys. 56, 3463 (1970).

15. R. A. W. Johnstone, F. A. Mellow, and S. D. Ward, Int. J. Mass Spectrom. Ion Phys. 5, 241 (1970).

16. A. J. C. Nicholson, J. Chem. Phys. 39, 954 (1963).

17. V. H. Dibeler, R. M. Reese, and M. Krauss, Advan. Mass. Spectrom. 3, 471 (1966).

18. B. Boone, R. K. Mitchum, and S. E. Scheppele, Int. J. Mass Spectrom. Ion Phys. 5, 21 (1970).

19. a) P. Natalis, and J. L. Franklin, J. Phys. Chem. 69, 2943 (1965); b) H. Budzikicwicz, C. Djerassi, and D. H. Williams, "Ass Spectra Of Organic Compounds", Holden-Day, San Francisco, Calif., 1967, Chapters 1 and 3.

20. G. G. Meisels and B. G. Giessner, Int. J. Mass Spectrom. Ion Phys. 7, 489 (1971).

21. J. F. Arnett, G. Newkome, W. L. Mattice, and S. P. McGlynn, J. Amer. Chem. Soc. 96, 4385 (1974).

22. W. A. Chupka and J. Berkowitz, J. Chem. Phys. 32, 1546 (1960).

23. W. A. Chupka and M. Kaminsky, J. Chem. Phys. 35, 1991 (1961).

24. a) G. G. Meisels, R. H. Emmel, S. E. Scheppele, K. F. Kinneberg, and J. A. Draeger, Advan. Mass Spectrom. 6, 955 (1974); b) S. E. Scheppele, R. K. Mitchum, J. A. Draeger, and G. Prakash, Proc. 22nd Annual Conf. Mass Spectrom. Allied Topics, Philadelphia, May 1974.

25. This compound was kindly prepared by Mr. Patrick L. Grizzle and Mr. Gil J. Greenwood, Dept. of Chemistry, Oklahoma State University.

26. S. E. Scheppele, Patrick L. Grizzle, and Dwight Miller, submitted for publication in the Journal of Organic Chemistry.

27. L. Fieser and M. Fieser, "Reagents for Organic Synthesis", Wiley, New York, N. Y., 1968, p. 1159.

28. J. Cason and F. S. Prout, "Organic Synthesis", Collect. Vol. 3, Wiley, New York, N. Y., 1955, p. 601.

29. I. Lalezari and M. Hatefi, J. Med. Chem. 14, 1138 (1971).

30. Preparation of this compound was done by Dr. R. K. Mitchum, while at the Dept. of Chemistry, Oklahoma State University.

31. C. D. Shacklett, and H. A. Smith, J. Amer. Chem. Soc. 75, 2654 (1953).

32. The LKB 9000P mass spectrometer was made available through Professor G. R. Waller.

33. G. G. Meisels, J. Y. Park, and B. G. Giessner, J. Amer. Chem. Soc. 92, 254 (1970).

34. I. B. M. System/360, Scientific Subroutine Package, Version III, 1968.

35. The numerical differentiation was performed by a program kindly provided by Professor L. M. Raff.

36. F. H. Field, and J. L. Franklin, "Electron Impact Phenomena and The Properties of Gaseous Ions", New. York. N. Y., Academic Press, 1957.

37. J. L. Franklin, J. Chem. Phys. 21, 2029 (1953).

38. R. K. Solly and S. W. Benson, J. Amer. Chem. Soc., 93, 1592 (1971).

APPENDIX A

THERMODYNAMICS OF FRAGMENTATION

The calculations of the ionization and appearance potentials for ions produced from benzil and 4-methoxybenzil-$\underline{d}_5$ by electron impact are given here. All values are in kcal/mole except where indicated. The deviation for each quantity in the calculations was its cited value, the average deviation, if more than one estimate was available, or assumed to be 5% of its value if the deviation was not available.

Benzil

The reported ionization potential for benzil is 8.78±0.20 eV.[19] Appearance potentilas of 9.70±0.20 eV and 15.12±0.20 eV for the benzoyl ion, m/e 105, and the m/e 77 ion, respectively, have been reported.[19]

An appearance potential of 15.36±0.7 eV has been calculated for the formation of m/e 77 from benzil according to Scheme II by Equation 4. The ΔH_f of m/e 77 is 285; the ΔH_f of CO is 26.42; and the ΔH_f's of

$$AP(m/e\ 77) = \{\Delta H_f(m/e\ 77) + \Delta H_f(CO) + \Delta H_f(C_7H_5O) - \Delta H_f(benzil)\}/23.06 \quad (6)$$

C_7H_5O and benzil are 21.0±2.0 and -21.8, respectively.

An appearance potential for the m/e 51 ion calculated from Equation 7 is 18.89±0.7 eV. The ΔH_f's of m/e 51 and C_2H_2 are 307 and

$$AP(m/e\ 51) = \{\Delta H_f(m/e\ 51) + \Delta H_f(C_2H_2) + \Delta H_f(CO) + \Delta H_f(C_5H_7O) - \Delta H_f(benzil)\}/23.06 \quad (7)$$

54.19.[19]

4-Methoxybenzil-d_5 (I)

The ΔH_f of I, has not been determined experimentally, and was estimated as follows. The $\Delta\Delta H_f$ for replacement of a p-hydrogen with a methoxy group was estimated to be -36.0 from the ΔH_f of 4-methoxyacetophenone (-57.0) and acetophenone (-23.0), 4-methoxybenzophenone (-23.9) and benzophenone (12.5), and 4-methoxybenzaldehyde (-48.1) and benzaldehyde (-10.5).[36] The ΔH_f of I is then computed to be -57.8±1.21, which is in agreement with the value of -55.52 calculated by group equivalents method.[37]

Based on a value of 8.86±0.14 eV for the ionization potential of benzil and the ΔH_f of benzil, the ΔH_f of its molecular ion is calculated to be 182.5±3.6 kcal/mole. The $\Delta\Delta H_f$ for the replacement of a p-hydrogen by a methoxy group was estimated to be -52.67 from the ΔH_f of the molecular ions of 4-methoxybenzophenone (178) and benzophenone (228), 4-methoxyacetophenone (142) and acetophenone (191), and 4-methoxybenzaldehyde (150) and benzaldehyde (209).[36] Thus, ΔH_f (II) is estimated to be 129.8±2.25 kcal/mole. The ionization potential of I is computed to be 8.14±0.20 eV.

The appearance potential of III was calculated by Equation 8. Equation 8 is applicable for the formation of III via Scheme I.

$$AP(III) = \{\Delta H_f(III) + \Delta H_f(C_7H_5O) - \Delta H_f(I)\}/23.06 \qquad (8)$$

Using a value of 26.1±2.0 for ΔH_f of the benzoyl radical[38] and a value of 128.7±2.0 for the ΔH_f of III from the ΔH_f(IV) and a ΔH_f(I) of -53, a value of 9.22±0.30 eV was calculated.

The appearance potential for IV via Scheme I is computed from Equation 9.

$$AP(IV) = \{\Delta H_f(IV) + \Delta H_f(C_8H_7O_2) - \Delta H_f(I)\}/23.06 \quad (9)$$

A value of 182.2±3.1 was taken as the $\Delta H_f(IV)$.[19] A value of -8.4±2.6 was estimated for the $\Delta H_f(C_7H_8O_2)$ from the ΔH_f of the benzoyl radical and the difference (-34.5) in the ΔH_f's of the 4-methoxybenzyl and benzyl radicals. The heat of formation of the 4-methoxyphenyl radical (36±2) was estimated from the difference of -34.5 and the phenyl radical (72±2). Equation 9 leads to a value of 10.35±0.30 eV.

APPENDIX B

STANDARD DEVIATIONS IN FDIE AND SDIE

Equation 10 was used in the calculation of the theoretical standard deviations in dI/dE.[36]

$$\sigma^2_{true}(FDIE) = \{\frac{K\ n\ R_b\ e\ \omega_e^2}{(\omega_m^2 + \omega_e^2)\ Tint}\}\ \{1 + \frac{\sigma_m^2}{n^2}\}\ \{1 + \frac{RC}{Tint} + \frac{RC}{Tint}\ \exp-\frac{Tint}{RC}\} \quad (10)$$

Values used in the calculation were K= 1.030, $R_b = 1.1 \times 10^8$ ohms, e= 1.6022×10^{-19} C, $\omega_e/2$= 660 Hz, $\omega_m/2$= 600 Hz, and $(1+\sigma m^2/n^2)$= 1.92. $(1+\sigma m^2/n^2)$ represents the contribution to the noise from the electron multiplier. The integration time is Tint, RC stands for the LIA time constant, and n is the multiplier gain.

The standard deviation in SDIE was calculated from Equation 11.

$$\sigma^2(SDIE) = \frac{1}{h}\ \{(F''(Vi)\ \sigma_h)^2 + 0.015787\ (\frac{\sigma(yi)\ yi}{100})^2\} \quad (11)$$

where F"(Vi) is the SDIE value at voltage Vi, h is the increment in the electron voltage, $\sigma(y_i)$ is the standard deviation in FDIE at voltage Vi, and y_i is the value of dI/dE at this voltage. The standard deviation in dI/dE is assumed constant over the range of dI/dE values required to calculate the d^2I/dE^2 value.

All calculations using ion current or derivatives were converted from counts per unit time to lock-in-amplifier voltage input. The counts per unit time were divided by M/ 2 times the frequency response

of the electron multiplier, where M is the modulation voltage and equals 0.032 volts and the frequency response is 0.74.

The convergence of σ_{true} and σ_{est} is shown in Figure 34. From the curve it is seen that 55 dI/dE points at a time constant of 30 seconds will converge to 96% of σ_{true} and 170 points at a time constant of 100 seconds will converge to 95% of σ_{true}. The relation of σ_{true} and σ_{est} is given in Equations 12 and 13.

$$\frac{\sigma^2_{est}}{\sigma^2_{true}} = 1 - \frac{2\ L}{n(n-1)} \tag{12}$$

$$L = \frac{2\ RC\ (\sinh \frac{Tint}{2\ RC})^2}{Tint-RC+RC\ \exp - \frac{Tint}{RC}} \times \frac{n-1+(\exp- \frac{nTs}{RC})-n\ \exp-\frac{Ts}{RC}}{(1 - \exp -\frac{Ts}{RC})^2} \times \exp- \frac{Ts}{RC} \tag{13}$$

where RC is the time constant, n is the number of dI/dE points, Ts is the time between successive dI/dE points, and Tint is the integration time.

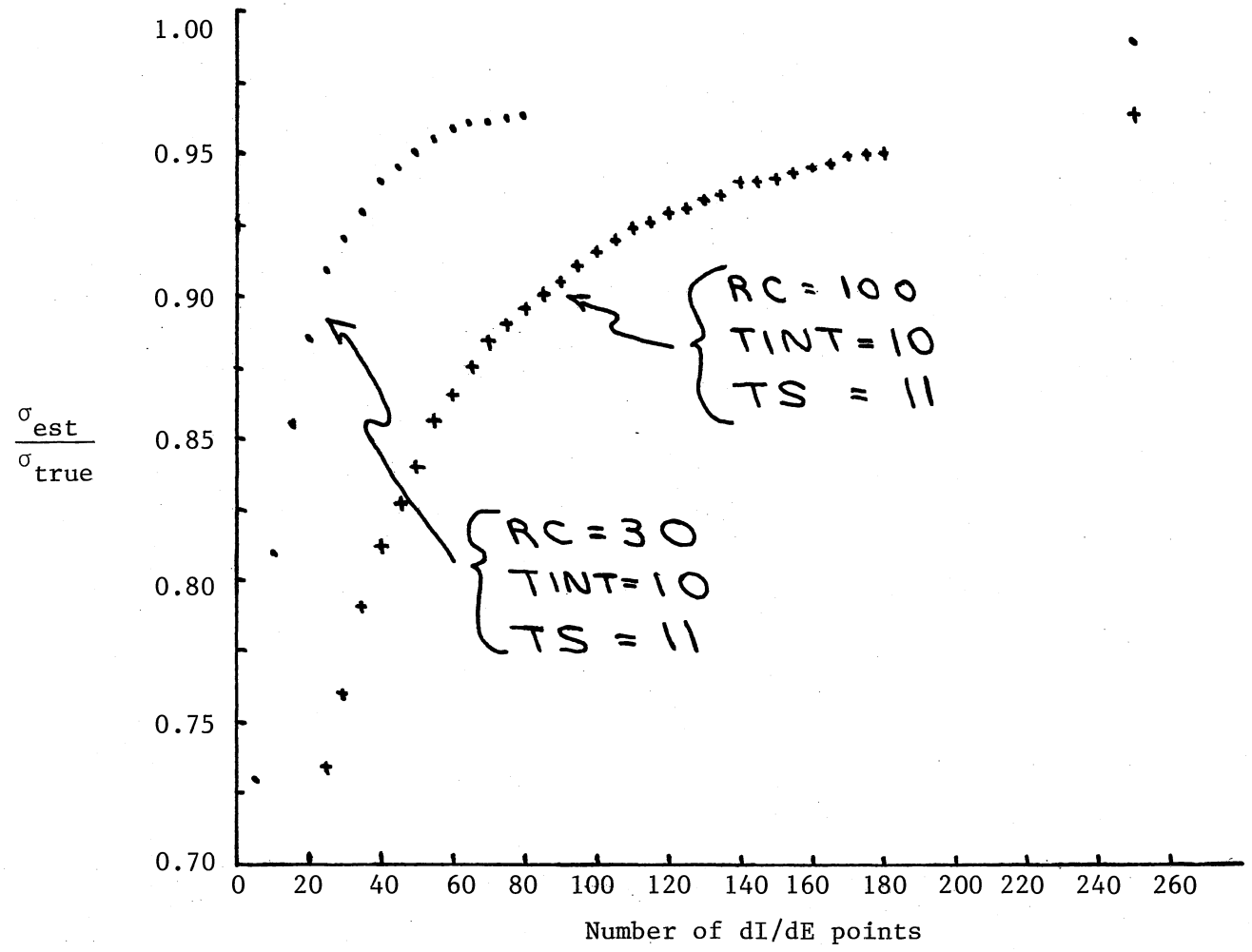

Figure 34. Convergence of σ_{est} to σ_{true}

APPENDIX C

PROGRAM FOR EVALUATION OF dI/dE

A program has been written for the evaluation of the experimental dI/dE values. The program is written in FORTRAN IV compiler language. The program contains 785 cards, uses 99K bytes of core in the compile step and 63K bytes in the go step. Up to 198 values for dI/dE may be processed.

A logic diagram for the program appears in Figure 35. The program is divided into five routines:

a) MAIN, reads in data and calls subroutines

b) INTG, numerically integrates FDIE and SDIE curves by Simpsons rule

c) INTEP, numerically interpolates values in SDIE

d) PLTS, plots I(E), FDIE, and SDIE using calcomp plotter

e) PL, line plots I(E), FDIE, and SDIE in output

The data for the program is arranged in the following manner. The first card has the name of the calibrating gas in columns 1-8, the measured ionization potential in columns 9-18, and the known ionization potential in columns 19-28. The second card contains the title and information concerning the ion. Card number three contains thirteen enteries concerning the use of subroutines and normalization factors. The dI/dE data appears following cards in format 11F6.0. More than one data set may be processed at a time. Two blank cards after the last

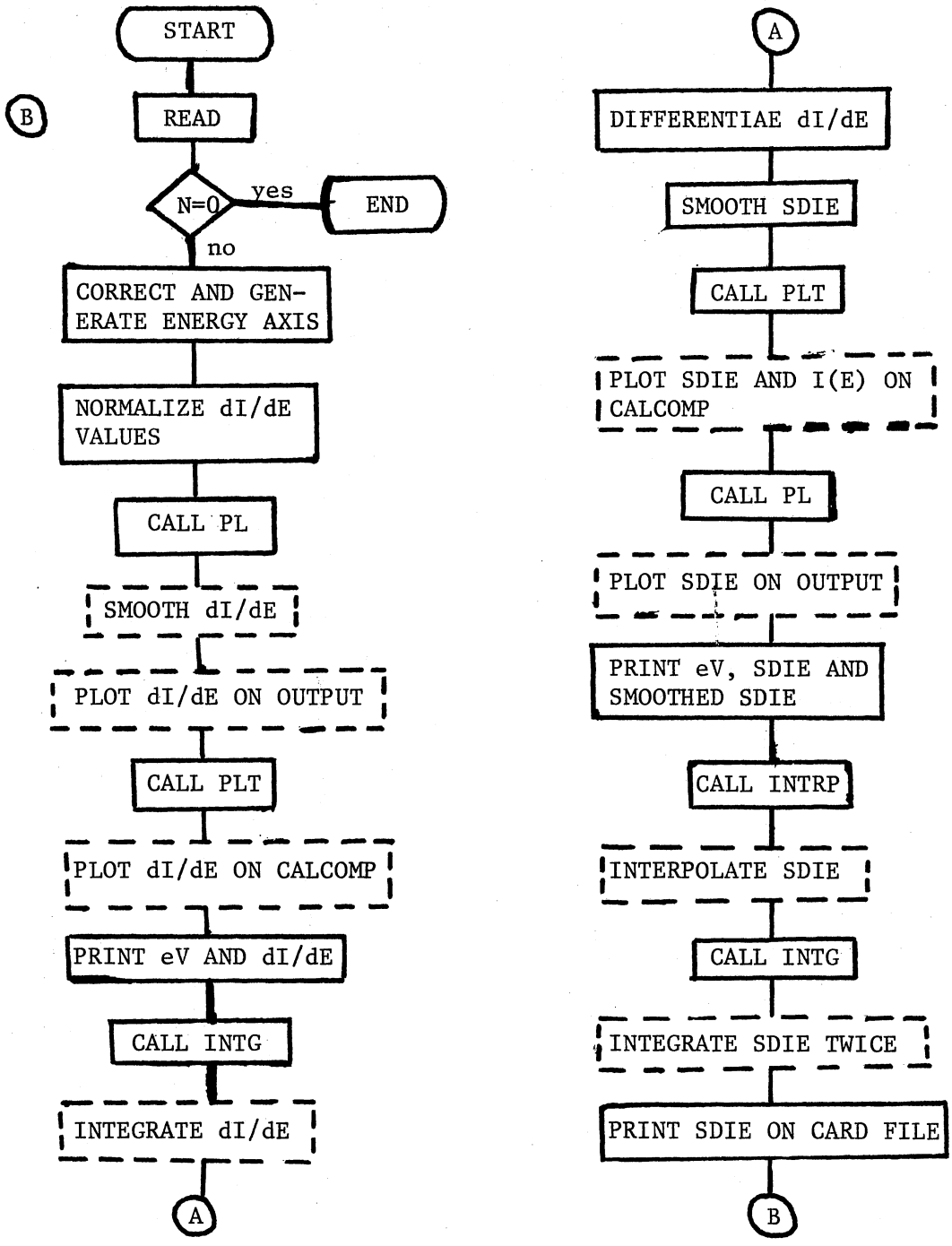

Figure 35. Logic Diagram for dI/dE Program

ion data set terminates the program properly. A list of the enteries for the control card (card three) are given in Table XI.

The program requests 110K bytes of computer core. Compiling time is 21.17 seconds. Execution of one ion requires approximately 0.00359 hours of processor time ($1.08), and 0.3890K byte-hours of processor storage ($0.29). Total cost is approximately $2.15 per ion.*

* Based on current rates on IBM 360/50 with calcomp plotter at the Oklahoma State University Computing Center.

TABLE XI

FORMAT FOR CONTROL CARD

Entry	Columns	Type[a]	Information
1	1-3	I	Number of dI/dE values
2	4-7	I	Increment of electron energy
3	8-13	F	Experimental I. P. of the molecule
4	14-19	F	Correction factor for LIA sensitivity
5	20-25	F	Starting value of electron energy
6	29-31	I	Number of smoothings FDIE
7	32-34	I	Number of smoothings SDIE
8	35-37	I	Plot of FDIE (enter 1)
9	38-40	I	Plot of SDIE (enter 1)
10	41-43	I	Integration (enter 1)
11	44-46	I	Interpolation (enter 1)
12	50-57	F	Normalization factor
13	61-63	I	SDIE cards (enter 1)

[a]I indicates integer, F indicates floating point number

APPENDIX D

CALCULATION OF ION INTENSITIES

The calculation of ion intensities from the breakdown graph and the appropriate energy deposition function is given here. The ion intensities are given by Equation 14.

$$V_k = \int_{E=IP}^{IP+Ei} \frac{SDIE\ (K)_{Ei}}{\sum_{J=I}^{N} SDIE\ (J)_{Ei}} P(ED)_{Ei,V}\ dE \qquad (14)$$

From Equation 3, the ion intensities may be given from Equation 15.

$$P(ED)_{Ei,V} = \sum_{J=I}^{N} SDIE\ (J)_{Ei} \times (V-E) \qquad (3)$$

$$V_k = \int_{E=IP}^{IP+Ei} \frac{SDIE\ (K)_{Ei}}{\sum_{J=I}^{N} SDIE\ (J)_{Ei}} \sum_{J=I}^{N} SDIE\ (J)_{Ei}\ (V-E)\ dE \qquad (15)$$

Equation 15 reduces to Equation 16.

$$V_k = \int_{E=IP}^{IP+Ei} SDIE\ (K)_{Ei}\ (V-E)\ dE \qquad (16)$$

VITA

Jon Alan Draeger

Candidate for the Degree of

Master of Science

Thesis: FRAGMENTATIONS OF AND ENERGY DEPOSITION IN MOLECULAR IONS OF 4-METHOXYBENZIL-d_5 AND BENZIL PRODUCED BY ELECTRON IMPACT

Major Field: Chemistry

Biographical:

Personal Data: Born in Sapulpa, Oklahoma, on June 28, 1949, one of four children of Harold M. and Fern E. Draeger.

Education: Graduated from Sapulpa High School, Sapulpa, Oklahoma, in 1967; received Bachelor of Science degree from Northeastern Oklahoma University, Tahlequah, Oklahoma, with a major in Chemistry, in July, 1971; completed requirements for the Master of Science degree July, 1975.

Professional Experience: Undergraduate Research Program Participant, University of Arkansas, summer 1970; Dow Chemical Fellow, summer 1974; Graduate Research Assistant, Oklahoma State University, 1975; Graduate Teaching Assistant, Oklahoma State University, 1971-1974.

Membership in Honorary and Professional Societies: Member of Rho Theta Sigma, Honorary Scholastic Society; member of Kappa Mu Epsilon, Honorary Mathematics Society; member of the American Chemical Society; member of Phi Lambda Upsilon, Honorary Chemical Society.